

A SURVEY FOR INDUSTRIAL USES OF DISTILLER'S DRIED GRAINS WITH SOLUBLES (DDGS)

A Thesis  
Submitted to the Graduate Faculty  
of the  
North Dakota State University  
of Agriculture and Applied Science

By

Joshua Louis Haugsdal

In Partial Fulfillment  
for the Degree of  
MASTER OF SCIENCE

Major Department:  
Mechanical Engineering

October 2012

Fargo, North Dakota

North Dakota State University  
Graduate School

---

**Title**

A Survey For Industrial Uses of Distiller's Dried

---

Grains with Solubles (DDGS)

---

**By**

Joshua Louis Haugsdal

---

The Supervisory Committee certifies that this *disquisition* complies with North Dakota State University's regulations and meets the accepted standards for the degree of

**MASTER OF SCIENCE**

---

SUPERVISORY COMMITTEE:

Dr. Long Jiang

---

Chair

Dr. Chad Ulven

---

Dr. Xiangfa Wu

---

Dr. Dennis Wiesenborn

---

Approved:

11/8/2012

---

Date

Dr. Alan Kallmeyer

---

Department Chair

## **ABSTRACT**

The increase in demand for corn ethanol has caused an increase in distiller's dried grains with solubles (DDGS), which is a byproduct of ethanol production. DDGS is a cheap byproduct and is primarily used for livestock feed filler. DDGS contains oils and proteins from corn and in this research we showed that corn oil and proteins could be extracted with ethanol. Zein protein is the main protein in DDGS and has been shown to have good adhesive properties. This protein was used as a binder in biocomposites with the DDGS after extractions and soy protein isolate (SPI). Mechanical properties and water resistance of the composites were studied. A wood adhesive was also prepared using the zein and cellulose nano-fibrils (CNF) as the adhesive reinforcement. Rheological tests were performed to study the flow property of the adhesive. This research demonstrated the potential of DDGS to be used as a raw material for multiple value-added industrial uses.

#### **ACKNOWLEDGEMENTS**

I would like to acknowledge my advisor Dr. Jiang for all the help and direction he provided during my research. I would also like to thank David Gutschmidt and Michael Cronin for assisting me in some of the work. Finally, thanks to the North Dakota Corn Council for funding me through this period.

## TABLE OF CONTENTS

ABSTRACT.....	iii
ACKNOWLEDGEMENTS.....	iv
LIST OF TABLES.....	ix
LIST OF FIGURES.....	x
LIST OF ABBREVIATIONS.....	xiii
LIST OF APPENDIX FIGURES.....	xv
CHAPTER 1. INTRODUCTION.....	1
1.1.    DDGS Oil Extraction .....	1
1.2.    Zein Extraction .....	2
1.3.    Zein Structure .....	5
1.4.    Zein Films .....	10
1.5.    Zein Adhesive .....	11
1.6.    Rheology .....	12
1.6.1.    Zein Rheology.....	12
1.6.2.    Rheology of Ionic Liquid Containing Fibers or Cellulose.....	13
1.7.    DDGS Composites .....	15
1.8.    Zein Protein Composites .....	17
1.9.    Soy Protein Film Processing and Soy Protein Composites .....	18
1.10.    Purpose for This Research .....	20
CHAPTER 2. RHEOLOGY OF ZEIN PROTEIN AND ZEIN/CELLULOSE NANOFIBRILS SOLUTIONS AND ITS USE AS A WOOD ADHESIVE.....	24
2.1.    Introduction .....	24
2.2.    Materials and Methods .....	24
2.2.1.    Materials.....	24
2.2.2.    Processing.....	25
2.2.3.    Rheological Testing.....	27

2.2.4.	Mechanical Testing.....	27
2.2.1.	Microscopy.....	28
2.3.	Results and Discussion .....	28
2.3.1.	Rheology Results.....	28
2.3.2.	Zein and Zein/CNF Adhesive Results.....	33
2.3.3.	Microscopy.....	35
2.4.	Summary of Results .....	38
CHAPTER 3. SOY PROTEIN AND ZEIN PROTEIN COMPOSITES.....		40
3.1.	Introduction .....	40
3.2.	Materials and Methods .....	40
3.2.1.	Materials.....	40
3.2.2.	Processing.....	40
3.2.3.	Mechanical Testing.....	41
3.2.4.	Thermal Testing.....	42
3.2.5.	Microscopy.....	42
3.2.6.	Water Absorption.....	42
3.3.	Results and Discussion .....	42
3.3.1.	Compression Test Results.....	42
3.3.2.	Thermogravimetric Analysis.....	47
3.3.3.	Microscopy.....	49
3.4.	Water Absorption Testing .....	50
3.5.	Summary of Results .....	51
CHAPTER 4. DDGS AND ZEIN PROTEIN COMPOSITES.....		53
4.1.	Introduction .....	53

4.2.	Materials and Methods .....	53
4.2.1.	Materials.....	53
4.2.2.	Processing.....	53
4.2.3.	Mecanical Testing.....	54
4.2.4.	Thermal Testing.....	55
4.2.5.	Water Absorption.....	55
4.2.6.	Microscopy.....	55
4.3.	Results and Discussion .....	55
4.3.1.	Tensile Testing Results.....	55
4.3.2.	Thermogravimetric Results.....	58
4.3.3.	Microscopy.....	59
4.3.4.	Water Absorption Results.....	61
4.4.	Summary of Results .....	63
CHAPTER 5.	CONCLUSION AND FUTURE WORK.....	65
5.1.	Future Work .....	66
REFERENCES.....		68
APPENDIX.	OIL AND ZEIN EXTRACTION FROM DDGS.....	73
A.1.	Introduction.....	73
A.2.	Materials and Methods .....	73
A.2.1.	Materials .....	73
A.2.2.	Processing .....	73
A.3.	Results and Discussion.....	75
A.3.1.	Oil Extraction Results .....	75
A.3.2.	Zein Extraction Results .....	76

A.4. Summary of Results ..... 77



**LIST OF TABLES**

<u>Table</u>	<u>Page</u>
3.1: TGA Results for Initial Degradation Temperature (IDT), Percent Weight Loss, and Residual Weight of SPI/Zein Composites. ....	48
3.2: Apparent Diffusion Coefficient ( $D_A$ ) Values for Soy/Zein Samples.....	51
4.1: TGA Results for Initial Degradation Temperature (IDT), Percent Weight Loss, and Residual Weight of DDGS/Zein Composites. ....	58

## LIST OF FIGURES

<u>Figure</u>	<u>Page</u>
1.1. Hydrodynamic radii of zein in various ethanol solutions. <sup>10</sup> .....	5
1.2. Model put forth by Argos et al <sup>13</sup> for the structure of zein. ....	7
1.3. Mean hydrophobicity profile of zein against the residue numbers. SS represents the signal sequence, NTT is for the N-terminal tail, and 1-10 represent each repeat section. <sup>14</sup> .....	8
1.4. Two possible configurations of how the repeats look in zein. The white dots symbolize hydrophobic regions, while the asterisks are for polar regions, and the black dots show positions on the hexagonal network. <sup>14</sup> .	8
1.5. The zero shear viscosity values of the SF solutions as a function of SF concentration. <sup>23</sup> .....	14
1.6. Main products derived from DDGS and their potential uses.....	21
2.1. A TEM image showing networks of CNF.....	25
2.2. Wood bars used for adhesive lap-shear testing.....	26
2.3. The compressive jig used to make zein adhesive samples.....	27
2.4. Viscosity as a function of shear rate for pure zein solutions.....	29
2.5. Viscosity as a function of shear rate for .6% CNF and zein mixtures...	29
2.6. Viscosity as a function of shear rate for .8% CNF and zein mixtures...	30
2.7. Viscosity as a function of shear rate for 1% CNF/zein mixtures.....	30
2.8. Viscosity as a function of zein concentration showing deflection at the critical concentration. ....	31
2.9. Storage modulus curves of the zein/CNF mixtures with different CNF concentrations. ....	32
2.10. Loss modulus curves of zein/CNF mixtures with different CNF concentrations. ....	32
2.11. G' and G'' curve comparisons of zein/CNF mixtures with different CNF concentrations. ....	33
2.12. Complex viscosity of various zein/CNF mixtures.....	33
2.13. Tensile testing results of zein and zein + GA adhesives.....	34
2.14. Picture of the fracture surface of a wood adhesive specimen.....	34

2.15. Tensile testing results for various zein/CNF adhesives.....	35
2.16. SEM images showing the wood surfaces without pure zein adhesive (a) and the fracture surfaces of the 25% pure zein adhesive bond (b and c).....	36
2.17. SEM images of the fracture surfaces of zein/CNF adhesive bonds. Adhesive formulation: 1% CNF and 11% Zein.....	37
2.18. Representative stress and strain curves for zein and zein/CNF adhesives.....	38
3.1. SPI/zein composite obtained from compression molding at room temperature. ....	43
3.2. Compressive strength for samples made at room temperature. SPI/zein ratio: 90/10 and 85/15. ....	44
3.3. Modulus for samples made at room temperature SPI/zein ratio: 90/10 and 85/15. ....	44
3.4. Soy/zein protein composite compressed at 130 °C.....	45
3.5. Compressive strength of the composites compressed at 130 °C.....	46
3.6. Modulus of the composites compressed at 130 °C.....	46
3.7. Stress-strain curves of selected composites with fracture toughness indicated on the curves. ....	47
3.8. TGA and dTGA curves for a) 90/10 b) 85/15 ratio samples.....	48
3.9. SEM images showing morphological differences seen in 85/15 sample.....	49
3.10. The water absorption of compression molded soy/zein protein samples..	50
4.1. Compression molded DDGS/zein material.....	55
4.2. Strength and modulus values obtained from tensile testing of DDGS/zein composite materials. ....	56
4.3. Strength and modulus values obtained from tensile testing of DDGS/zein/flax fiber composite materials. ....	57
4.4. Representative stress and strain curves for DDGS/zein composite materials. ....	58
4.5. TGA and dTGA curves for DDGS/zein composite materials.....	59
4.6. SEM images showing fracture surfaces of an 85/15 DDGS/zein (a), 85/15 + Glycerol (b), 85/15 + PPG (c), and 85/15 + PPG + GA (d). ....	60

4.7. SEM images of fracture surfaces from DDGS/Zein/Flax fiber composites.  
a) 15wt% flax fiber b) 2wt% flax fiber c) 15 wt% flax fiber d) 2wt%  
flax fiber and samples were 85D/15Z+PPG+GA. .... 61

4.8. Water absorption vs. time curves for DDGS/zein composite material..... 62

4.9. Water absorption vs. time curves for DDGS/zein composite materials  
containing flax fibers. .... 63

## LIST OF ABBREVIATIONS

DDGS.....	Distiller's Dried Grains with Solubles
CGM.....	Corn Gluten Meal
CGF.....	Corn Gluten Feed
STS.....	Solvents-to-Solids
SDS-PAGE.....	Sodium Dodecyl Sulfate Polyacrylamide Gel Electrophoresis
HCl.....	Hydrochloric Acid
kDa.....	Kilo Dalton
CD.....	Circular Dichroism
SAXS.....	Small Angle X-Ray Scattering
R <sub>g</sub> .....	Radius of Gyration
R <sub>c</sub> .....	Cross-sectional Radius of Gyration
Wvp.....	Water Vapor Permeability
PPG.....	Poly (Propylene Glycol)
PEG.....	Poly (Ethylene Glycol)
ETB.....	Elongation to Break
GA.....	Glutaraldehyde
CA.....	Citric Acid
BTCA.....	Butanetetracarboxylic Acid
DAS.....	Dialdehyde Starch
BHT.....	Butylated Hydroxytoluene
RH.....	Relative Humidity
TEG.....	Tri (Ethylene) Glycol
EMIMc.....	1-Ethyl-3-Methylimidazolium Acetate
MC.....	Microcrystalline Cellulose
SSP.....	Spruce Sulfite Pulp
BC.....	Bacterial Cellulose

SF.....Silk Fibroin  
AmimCl.....1-Allyl-3-Methylimidazolium Chloride  
PLA.....Poly (Lactic Acid)  
MDI.....Methylene Diphenyl Diisocyanate  
FTIR.....Fourier Transform Infrared Spectra  
SEM.....Scanning Electron Microscopy  
DSC.....Differential Scanning Calorimetry  
TGA.....Thermogravimetric Analysis  
DMA.....Dynamic Mechanical Analysis  
T<sub>g</sub>.....Glass Transition Temperature  
PHBV.....Polyhydroxy(butyrate-co-valerate)  
PBS.....Poly (Butylene Succinate)  
PMDI.....Polymeric Methylene Diphenyl Diisocyanate  
SPI.....Soy Protein Isolate  
SPC.....Soy Protein Concentrate  
SS.....Sodium Sulfite  
CNF.....Cellulose Nano-Fibers  
IDT.....Initial Degradation Temperature  
LDPE.....Low Density Poly(Ethylene)  
PP.....Poly(Propylene)

**LIST OF APPENDIX FIGURES**

<u>Figure</u>	<u>Page</u>
A1. Oil extractions as functions of time and temperature.....	75
A2. Zein extractions as functions of time and temperature.....	76

## CHAPTER 1. INTRODUCTION

With the emergence of ethanol as an alternative fuel, the amount of Distiller's Dried Grains with Solubles (DDGS) has gone up from 26 million tons in 2007-08 to 39 million tons in the 2009-10 year and a total of 43 million tons produced in 2010-11 as presented by Wisner.<sup>1</sup> This increase has resulted in a surplus of a cheap byproduct with a price reported around \$210/ton or \$.11/lb by McFarland.<sup>2</sup> DDGS is currently most often used as filler in livestock feed and contains protein (24-27%), carbohydrates (39-62%), oils (3.5-13%), and ash (2-10%) as reported by Li and Sun.<sup>3</sup> Some of these constituents, if extracted, such as corn oil and zein protein, could add value to DDGS that would help make ethanol plants more profitable.

### 1.1. DDGS Oil Extraction

According to Shukla and Cheryan<sup>4</sup> zein makes up 35 to 60 percent of the protein in corn and the majority of zein is found in the endosperm region of the kernel. Corn oil is typically extracted from corn byproducts, such as corn gluten meal (CGM) and corn gluten feed (CGF), which are made from the wet milling process which also produces starch and corn oil.

Singh and Cheryan<sup>5</sup> extracted oil from DDGS using absolute ethanol. They held time and temperature constant but varied the ethanol to DDGS ratio from 2 to 10 ml/g. The results show that after a ratio of six, the amount of oil extracted becomes insignificant. During these extractions, some protein and glycerol was extracted but the amounts were less than 4 and 43 mg/g of DDGS, respectively.

Kwiatkowski and Cheryan<sup>6</sup> did a similar study with ground corn. They used previous work done by Kwiatkowski<sup>7</sup> to set the optimal time and temperature of 30 min and 50 °C. The solvents-to-solid (STS) ratio was increased from 2 to 8



ml/g. Finally, they determined whether it was viable to use old ethanol for extractions on new ground corn.

When looking at the STS, they found that the optimal value was 4 ml/g. This was determined based on extracted oil and recovery of solvent from the process. The multiple extraction study showed that after three repeats with new ground corn the amount of oil was minimal but there was still a large amount of material being extracted. This was due to the increased water content in the ethanol, which will cause other solids to be extracted, such as protein.

### **1.2. Zein Extraction**

The extraction of zein has been studied well and the following paragraphs discuss some work conducted to determine what process and solvents work. Typically zein is extracted in a process with aqueous alcohol in varying concentrations, but other solvents were studied to see the probability of or how well they could dissolve zein.

Selling and Woods<sup>8</sup> proposed using acetic acid as an improved solvent to dissolve zein from CGM and other sources. They investigated the effect time and temperature had on this process. The time study showed that after 120 minutes the amount of zein plateaued, while the temperature study showed there was a significant increase between 45 and 55 °C. They also determined from sodium dodecyl sulfate polyacrylamide gel electrophoresis (SDS-PAGE), the zein that was extracted is similar to commercially available zein and the composition of the zein did not change over time.

Xu et al<sup>9</sup> also looked at extracting zein not only under acidic conditions, but also under alkali conditions. Instead of using a pure acid or a pure base, they adjusted the pH of the ethanol solution with hydrochloric acid (HCl) or sodium hydroxide. They also studied the effects of adding

sodium sulfite to the solutions while varying time, temperature, and solvent to solids ratio. The pH part of the study showed increased amounts of zein was attained at both high alkaline and acidic conditions but the highest amount was achieved at a pH of one and two. Severe hydrolysis occurred at a pH of one which resulted in a lower viscosity zein solution. The zein acquired at a pH of two would be the better result as it would be a higher molecular weight. They found that after 20 minutes, the amount of zein reached its maximum value of 10% and as temperature was increased up to the boiling point, ethanol zein extraction amounts increased steadily to 10%. The maximum solvent to solids ratio was determined to be around a ratio of 10:1 or 12:1. Finally, the results from adding sodium sulfite showed that an addition of 0.25% increased the extracted zein amount, but anything over 0.25% was decreased slightly. The increase was attributed to the ability of sodium sulfite to break disulfide bonds.

Both of the previous papers discuss methods deemed successful at extracting zein from different source material and either not using an alcohol or changing the alcohol greatly. The main method of using aqueous alcohol is one that would prove most useful for extraction of zein from DDGS as it would be readily available at the ethanol plants.

Parris and Dickey<sup>10</sup> conducted research to study what the effects of changing the ratio between ethanol and water had on the extracted zein. They did this by using SDS-PAGE on solutions ranging from 50 to 95% ethanol. This showed that at higher ethanol percentages, the zein was primarily  $\alpha$ -zein, which has a molecular weight around 22 and 24 kDa, but as you moved towards 70 and 80 % ethanol, the zein started to contain  $\beta$ -zein, which has a molecular weight around 18 kDa. Finally, as the ethanol percentage approached 50 and 60 % the zein that was extracted contained small amounts of  $\alpha$ -zein and

$\beta$ -zein, but also had some  $\delta$ -zein, which has a molecular weight around 10 kDa. Meanwhile, they determined what affect the addition of sulfuric acid, lactic acid plus sulfur dioxide, sodium bisulfite, and sodium sulfite had on the extraction process. Lactic acid plus sulfur dioxide had the largest yield at 2.7 % and formed a film that had the highest strength and elongation to break, but the lowest modulus. The sodium bisulfite had the lowest yield of zein at 1.3 %, while sodium sulfite produced a film with the lowest strength and elongation to break.

Lawton<sup>11</sup> also used ethanol but did not add water. Instead, he put the solution in a heated pressure vessel and increased the temperature of the solution to 130 °C. This was allowed to stir for 30 minutes, after this time the solution was cooled and extracted. They used commercially available and hand collected CGM, corn grits, and DDGS in this experiment. Similar amounts of zein were extracted from both types of CGM, while the grits and DDGS had less extracted, which was expected as both contain less zein to start with. Next, they determined if defatting the CGM would result in an increase of extracted zein. This process helped with the commercial type, but not the hand collected CGM. Next, multiple runs were conducted to determine if more zein could be extracted after the initial extraction. This study showed a small amount was extracted the second time but repeated runs resulted in an insignificant amount removed. Finally, the operating temperature was reduced to 90 °C because the zein extracted at 130 °C was brownish-yellow in color. This reduction in temperature resulted in less zein being extracted, but the decrease may have been due to a change in the process during removal of the zein solution that probably left some in the reactor.

Kim and Xu<sup>12</sup> studied aggregation of zein in solutions ranging from 70 to 90% ethanol. Aggregation was determined by looking at the hydrodynamic radii

of zein. The data they acquired is shown in Figure 1.1. The decrease at 90% is attributed to a structural inversion of zein. Kim and Xu<sup>10</sup> describe it best, "zein aggregates form a micelle-like structure in which the hydrophilic moiety is oriented toward the solvent medium at lower than 90% ethanol and oriented toward the center of each aggregate at greater than 90% ethanol."

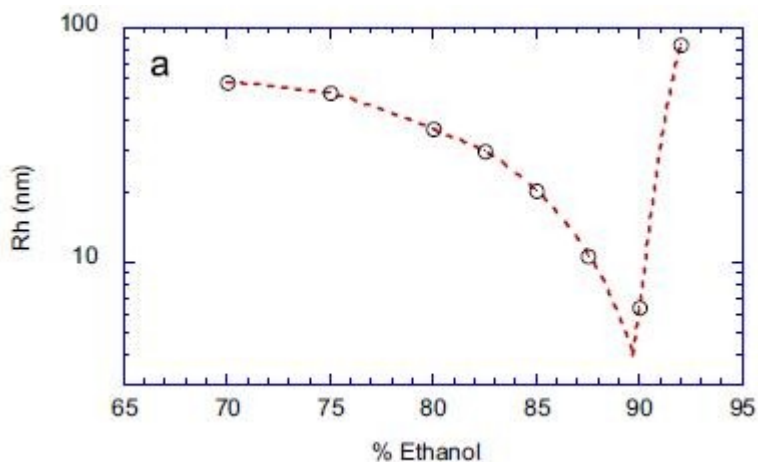


Figure 1.1. Hydrodynamic radii of zein in various ethanol solutions.<sup>10</sup>

They further showed this by putting glass spheres (hydrophilic) and toner (hydrophobic) into zein solutions. The zein was then precipitated out by either adding water to decrease ethanol, or by adding more ethanol. When water was added, the zein aggregated on the toner, but when ethanol was added, zein aggregated on the glass spheres. This experiment shows how zein aggregation changes by how much ethanol maybe present.

### 1.3. Zein Structure

Not only is it important to understand how to extract zein, but understanding the structure of the protein is also highly important. This structure can affect the characteristics of zein.

Argos et al<sup>13</sup> studied the structure of zein, specifically  $\alpha$ -zein, which consists of two weights: Z19 and Z22. They used Circular Dichroism (CD) and other tests to determine zein's physical characteristics. The CD data showed

that zein was 40 to 60%  $\alpha$ -helix and 50 to 40% reverse turn in nature; this was also previously shown with optical rotary dispersion testing. The other tests included four tests: 1. the experimental hydration potential 2. the Chou-Fasman conformation preference parameters for  $\alpha$ -helix 3. the Chou-Fasman conformational propensities values for reverse turn configurations 4. the normalized propensities for residue to be in a helical conformation within a membrane. When compared with experimental data, these parameters should show where the turns, which are glutamine rich, in the protein occur in the sequence of the residues. All the tests show good or decent agreement with the theoretical values, except for Chou-Fasman helical potential data but they do not elaborate on why it does not correlate. They then talk about how some residues in different helices join and form polar surfaces on the side of the helix. These faces are separated at  $120^\circ$  increments and lay at varying vertical positions. All these facts were considered and a model of the protein was formed. This model proposes that each helix forms a rod and then these rods are bonded by the polar faces in anti-parallel fashion which then form a non-circular cylinder. The turns would then make up the caps of the protein. The suggested model is seen in Figure 1.2.

Garret et al<sup>14</sup> expanded upon Argos et al.<sup>13</sup> while considering the genetic evolution of zein-like  $\alpha$ -prolamins from various plants. They used statistical analysis to evaluate relationships between different sequences and the alignment of the sequences. They also used a hydrophobicity test similar to what Argos et al.<sup>13</sup> used to study the helices. The only weight that was considered was Z22 as the most of the other plants do not contain Z19.

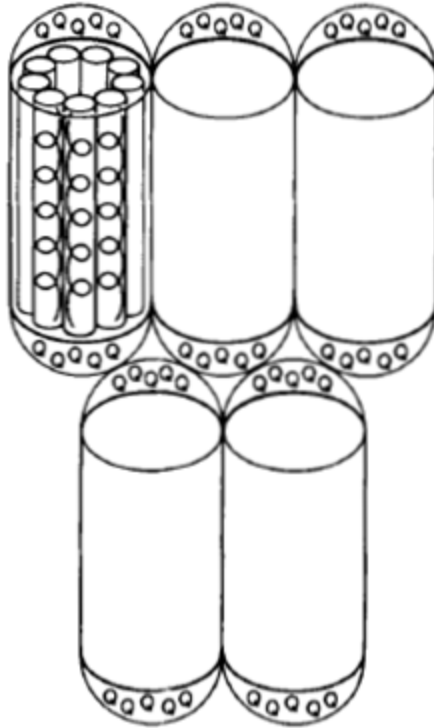


Figure 1.2. Model put forth by Argos et al<sup>13</sup> for the structure of zein.

The statistical analysis helped align the sequences and showed where the turns occurred, thus defining each repeat of the protein. This also helped to establish the tenth repeat in the series. The analysis was also used to establish that repeats 3, 5, and 7 are related, while repeats 4, 6, and 8 are associated. The hydrophobicity profile shown in Figure 1.3 shows that repeats 3 through 8 occur in pairs (i.e. 3 and 4, 5 and 6, and finally 7 and 8), and also shows that all the odd repeats show a greater propensity to form helices.

When they propose their model, they agree that the helices form in antiparallel fashion and have polar and hydrophobic faces separated by  $120^\circ$ . Instead of them forming a non-circular cylinder though, they suggest the helices pack next to each other following a hexagonal net as seen in Figure 1.4.

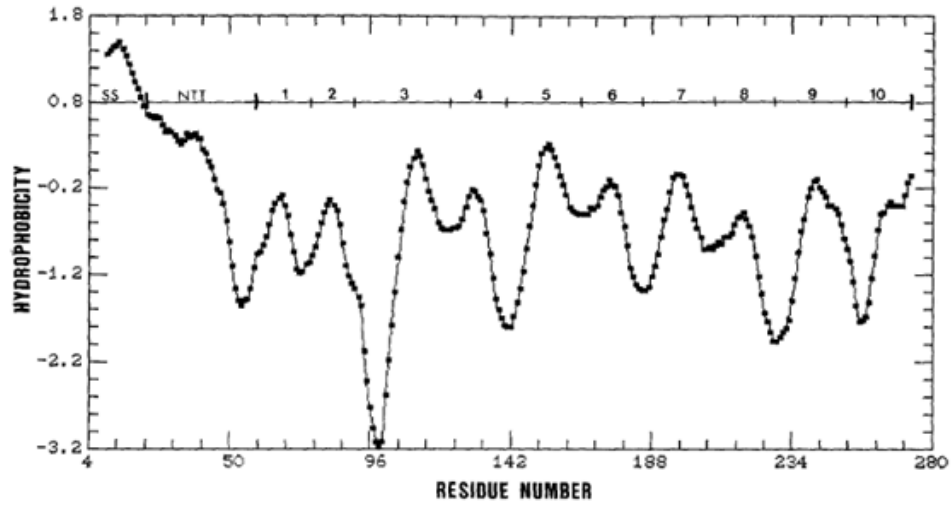


Figure 1.3. Mean hydrophobicity profile of zein against the residue numbers. SS represents the signal sequence, NTT is for the N-terminal tail, and 1-10 represent each repeat section.<sup>14</sup>

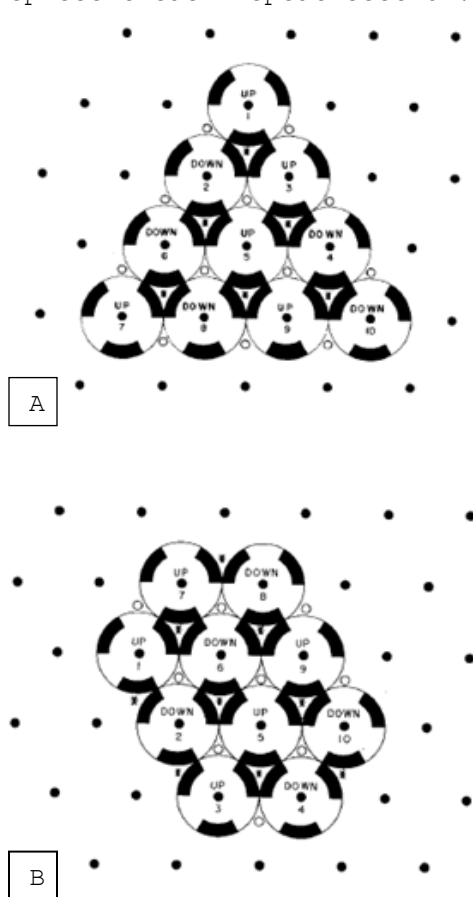


Figure 1.4. Two possible configurations of how the repeats look in zein. The white dots symbolize hydrophobic regions, while the asterisks are for polar regions, and the black dots show positions on the hexagonal network.<sup>14</sup>

More recently, Matsushima et al<sup>15</sup> studied  $\alpha$ -zeins with small-angle X-ray scattering (SAXS). This analysis can determine the overall radius of gyration ( $R_g$ ) and also the cross-sectional radius of gyration ( $R_c$ ) if one dimension is larger. They varied the protein concentration from 2 to 40 mg/ml and also added  $\beta$ -mercaptoethanol (.1 and 2%) to try and ensure that they had monomers and not dimers or oligomers.  $R_g$  varied for both concentrations of  $\beta$ -mercaptoethanol from 4.1 to 3.6 nm in a decreasing linear fashion as zein concentration increased. Similarly, the pure zein solution started at 5 and decreased to 4.3 nm.  $R_c$  also varied for both  $\beta$ -mercaptoethanol concentrations from 1.4 to 1.2 nm in a decreasing fashion, while the pure zein solution decreased from 1.9 to 1.4 nm. They suggested that zein may take the form of a sphere,  $\alpha$ -helix rod, random coil, or worm like chain, but when comparing theoretical values for these shapes, they did not match the experimental ones obtained. Finally, they proposed that zein took a rectangular prism form with dimensions  $a \times b \times c$ . They related  $a$  to  $R_g$  and  $R_c$  by the first equation

$$a^2 = 12(R_g^2 - R_c^2)$$

and  $R_c$  is related to  $b$  and  $c$  by the following equation.

$$R_c^2 = \frac{1}{12}(b^2 + c^2)$$

After calculating using  $a = 13$  nm,  $b = 1.2$  nm, and  $c = 3$  nm an  $R_g$  of 3.9 nm and  $R_c$  of 1 nm were obtained. The  $R_g$  value fits with the experimental values obtained, but the  $R_c$  value is slightly smaller. This was attributed to oligomers and by adjusting the value of  $b$  to 4.2 nm to account for this,  $R_g = 4.0$  nm and  $R_c = 1.5$  nm, which fits better with experimental results.



#### 1.4. Zein Films

Zein has been pursued as films for use in a variety of applications; the food industry has looked for green alternatives to current synthetic based films. Zein would fill this roll well since it is renewable and decomposes, but further research is necessary to improve its properties.

Parris and Coffin<sup>16</sup> used zein cast films with solutions prepared in ethanol or acetone. Both of these films were extremely brittle, thus they tried adding plasticizers and crosslinkers to improve the film's mechanical properties. They also considered how these additives would affect the water vapor permeability (wvp). The plasticizers poly (propylene glycol) (PPG), poly (ethylene glycol) (PEG), and glycerol were each added separately and PPG and PEG were combined with glycerol in varying ratios. The addition of each plasticizer separately had little effect on mechanical properties, but did reduce their wvp properties. The combination of glycerol and PEG did little to improve mechanical properties for the film, but glycerol and PPG in a 1:3 ratio increased the properties of the film. Elongation at break (ETB) increased almost 50 times when compared to films plasticized by glycerol.

Crosslinkers that were added consisted of formaldehyde, glutaraldehyde (GA), epichlorohydrin, citric acid (CA), and butanetetracarboxylic acid (BTCA). Formaldehyde in ethanol films showed the highest tensile strength, while all the acetone prepared films had the lowest tensile strength values. These results are the reason the acetone films were left out when plasticizers were added to the crosslinked solutions. All crosslinked and plasticized films had lower tensile strength than the pure crosslinked films and the 1:3 mixture of glycerol to PPG consistently had the lowest tensile strength, but the highest ETB. Finally, polymeric dialdehyde starch (PDS) was

added as a crosslinker. These films showed higher tensile strengths than pure zein films. PDS was the only additive that improved the wvp of the films.

Spence et al<sup>17</sup> also conducted work with dialdehyde starch (DAS) and zein films. They looked at what effects on the films, changes of different oxidation levels of DAS, ratio of DAS to zein, and the addition of water and glycerol as plasticizers would have. The oxidation of the DAS was varied from 0 to 90% and caused the tensile properties to increase as 90% was approached. The water absorption also decreased as the oxidation level increased. This is thought to be due to the increased amount of crosslinking happening between DAS and zein. As the ratio between DAS and zein was decreased to 1:1 from 9:1, the water absorption increased and the tensile properties decreased. Water caused the tensile properties of the films to decrease as it was varied from 9.3 to 12%, but the water absorption decreased. Finally, they added butylated hydroxytoluene (BHT) and sodium bisulfite. BHT caused little effect on the DAS and zein films. Sodium bisulfite on the other hand caused the tensile properties to decrease as it was varied from 0 to 5%, and the water absorption increased over that span. This was thought to be due to the sodium bisulfite interacting more with the DAS and not allowing it to crosslink with zein.

### **1.5. Zein Adhesive**

Zein's ability at binding allows it to be used as an adhesive. An initial patent <sup>18</sup> proposed to use zein as an adhesive for non-fibrous material. In the end, zein lost out to synthetic adhesives with better properties.

Recently though, Parris and Dickey<sup>19</sup> studied zein for use as a water resistant adhesive. They put two different zein solutions, a zein-lipid (zein concentrate) and commercial zein, with zein varying from 1 to 20%, between

glass slides in a lap-shear orientation to determine the film's mechanical properties. The pHs of the solutions were also adjusted to an acid and alkali level to see if this improved its adhesive abilities. The films were stored at 29 and 52 % relative humidity (RH) to simulate different conditions that it may have to perform under. Of the straight zein solutions, the commercial zein at 20% zein performed the best at 29 % RH with a load around 800 N, while the zein concentrate at 20 % zein reached only about 700 N. At 52% RH, the zein concentrate, again at 20 % zein, increased to almost 800 N and the commercial zein at 20% zein decreased to about 400 N. They also introduced PEG into the adhesive and varied it from 0 to 30%. The maximum load was achieved with a PEG content of 10%. Finally, adjusting the pH to an acid or alkali did not improve the performance of the adhesive over that of the regular zein solutions.

## **1.6. Rheology**

The concentration of zein in the solvent can have a large effect on the elastic and fluid behavior of the solution. Also, the introduction of nanoparticles and fibers can affect the flow behavior of the fluid.

### **1.6.1. Zein Rheology**

Selling et al<sup>20</sup> studied the effects that water and tri (ethylene) glycol (TEG) had on zein to see if they would improve the ease of processing. Water was varied from 5 to 30% and TEG 10 to 30%. As water content increased, the initial torque decreased, but as water content passed 10%, a rapid rise in torque was observed after mixing. When the water content passed 15%, another rise in torque was observed after the initial rise, at a later time in the mixing, as the amount of water approached 30% that seconded increase occurred after a shorter period of time. The TEG also decreased initial torque as its content increased. No increase in torque was observed over the mixing period

of 20 minutes. To induce the rapid rise in torque, temperature of the mixing pot was varied from 75 to 120 °C. The rapid rise in torque occurred for a temperature of 120 °C. In a combination containing 17% TEG and varying amounts of water, the initial torque is reduced and the rapid rise in torque is only seen after 3.9% water is added.

Zhang et al<sup>21</sup> studied how adjusting the pH of zein solutions to either acidic or basic levels affected the rheological properties. Zein in 70% ethanol solutions had their pH adjusted to 2.7, 3.3, 6.5 (neutral), 10.5, and 12.5. After conducting rheological studies, it was shown that the neutral solution had the highest viscosity. This change was attributed to the treatments causing zein to unfold some, thus reducing polymerization and aggregation. The solutions showed a shear thinning behavior and this was verified by analyzing the data with the Ostwald-de Waele model. This model confirmed that they were shear thinning and the most acidic and basic solutions were closest to Newtonian behavior. Finally, dynamic testing showed the solutions were more elastic as  $G'$  is normally larger than  $G''$  and that the pH adjustment had a drastic change on the viscoelastic properties.

#### **1.6.2. Rheology of Ionic Liquid Containing Fibers or Cellulose**

Gericke et al<sup>22</sup> studied the rheological properties of cellulose in 1-ethyl-3-methylimidazolium acetate (EMIMAc), which is an ionic liquid. They used microcrystalline cellulose (MC), spruce sulfite pulp (SSP), and bacterial cellulose (BC) for different types of cellulose. Steady state analysis showed that over most of the region chosen the fluid behaved in a Newtonian fashion and only showed slight non-Newtonian behavior at high shear rates and concentrations. It was also observed that as temperature increased the viscosities of the solutions decreased. Relative viscosity was studied as a function of cellulose concentration. This showed that as concentration

increased so did viscosity, but it also shows that as temperature increased there was less of a viscosity increase. Intrinsic viscosity also decreased with increasing temperature. All of these viscosity decreases were not due to decomposition of the cellulose but, was believed to be due a degradation of EMIMAc.

Similarly, Wang et al<sup>23</sup> studied the rheological properties of silk fibroin (SF) in 1-allyl-3-methylimidazolium chloride (AmimCl). Viscosity increased as SF content increased. Initially at small or no SF content and low shear rates the fluids would show shear thinning behavior. This behavior disappeared as SF content increased and then started to show up at high SF content and high shear rates. A graph showing the zero shear viscosity values for SF as a function of SF concentration is seen in Figure 5 below. Subset a of Figure 1.5 shows how the particles in the solution do not interact a lot with each other in the dilute region. The point where particles start to interact with each other is the critical concentration, which was determined to be 5% of SF, this increase in interaction results in an increase in viscosity. After that point the particles become more entangled, causing the viscosity to increase even more.

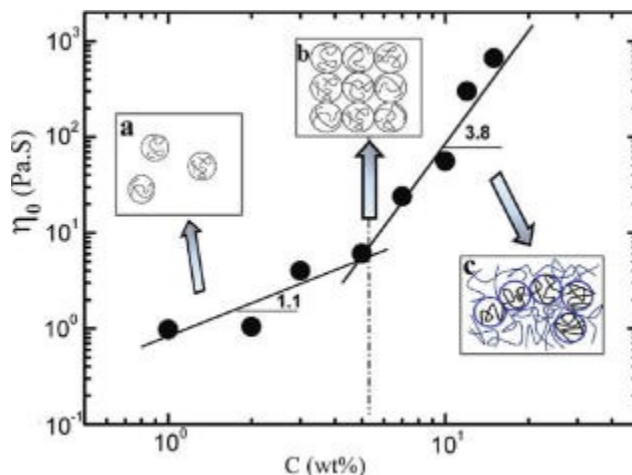


Figure 1.5. The zero shear viscosity values of the SF solutions as a function of SF concentration.<sup>23</sup>

The initial shear thinning at low SF concentrations and shear rates, along with the shear thinning at high SF concentrations and shear rates were analyzed. The initial shear thinning was thought to be due to the solvent, as there is a possibility that hydrogen bonding may occur in it. On the other hand, this shear thinning happening at high concentrations and shear rates is probably more due to the alignment of SF.

### **1.7. DDGS Composites**

DDGS as previously stated, is used mainly for use as filler in livestock feed, but DDGS has also been looked at for use in composite materials. Since it is currently a cheap product, its main purpose in composites would be as filler material.

Tatara et al<sup>24</sup> studied the effects of adding DDGS to phenolic resin. All samples were processed by compression molding and DDGS was added in varying concentrations up to 90%. Tensile testing was conducted to determine what effect the filler had on the mechanical properties of the resin. This showed that as the DDGS content was increased yield strength, modulus, and elongation to break (ETB) decreased. Yield strength was decreased by 76% with 90% DDGS, while modulus was decreased by 60% and ETB was 42%.

Li and Sun<sup>25</sup> created a composite material out of poly (lactic acid) (PLA) and DDGS. They also used methylene diphenyl diisocyanate (MDI) as a coupling agent to try and improve the composites properties. PLA was mixed with 20 to 50% DDGS and then a PLA and 20% DDGS had 0.25 to 2% MDI added. They conducted tensile testing, Fourier-transform Infrared Spectra (FTIR), scanning electron microscopy (SEM), differential scanning calorimetry (DSC), Thermogravimetric analysis (TGA) and dynamic mechanical analysis (DMA). Tensile testing for samples without MDI showed that any added DDGS decreased strength and modulus, but increased ETB with the maximum occurring at the 10%

DDGS loading. When MDI was added to the PLA and 20% DDGS, it increased the materials properties over that of not having any MDI and reached values similar to plain PLA with 1% MDI added. SEM imaging showed that MDI helped PLA adhere to the DDGS, which helps explain the improvements when MDI was added.

DSC graphs showed that the addition of DDGS decreased  $T_g$  by 3 °C, when compared to just PLA, but when MDI was added it started to increase  $T_g$  back. TGA showed that the inclusion of DDGS increased remaining residual weight and increased decomposition temperatures slightly. While MDI addition brought the decomposition temperatures back down slightly. Finally DMA showed that samples without MDI had a lower storage modulus ( $E'$ ). Also the loss factor ( $\tan \delta$ ) showed a  $T_g$  of 69 °C and that the pure PLA was more amorphous than the composites containing DDGS.

Zarrinbakhsh et al<sup>26</sup> similarly used DDGS as a filler in a matrix of Polyhydroxy (butyrate-co-valerate) (PHBV) with 30% poly (butylenes succinate) (PBS) added to increase the toughness, as PHBV is a brittle material. DDGS was added at 30% and either washed or not washed with water. Polymeric methylene diphenyl diisocyanate (PMDI) was added as a compatibilizer. They conducted TGA, tensile testing, SEM, HDT, and DMS to determine how much of an effective filler DDGS could be. TGA showed that addition of washed DDGS increased initial decomposition temperature over that of non-washed DDGS. This is because the water soluble material is removed during washing. Tensile testing showed that inclusion of non-washed DDGS decreases mechanical properties substantially. Washing somewhat improves properties over non-washed, but it is still not as high as the pure polymer matrix alone. The addition of PMDI returns properties to the same level, or a little higher than the polymer matrix. SEM shows that interfacial adhesion was improved

with washing and the addition of PMDI. DMA of the composite was improved with the addition of washed DDGS and PMDI, but was reduced with non-washed DDGS. Finally, HDT was again reduced by the addition of non-washed DDGS, but returned to original levels with the washed DDGS and was actually improved when compatibilizer was added.

### **1.8. Zein Protein Composites**

Zein has shown capabilities of acting as an adhesive. This property has led some people to try using zein to modify fibers in composite material to achieve better adhesion between the fiber and matrix. People have also tried to use zein as the matrix itself.

John and Anandjiwala<sup>27</sup> looked at using zein to modify flax fibers in a poly (propylene) matrix. Weight fraction of flax fibers was varied from 0 to 40%. Fibers were also treated in a solution of aqueous ethanol containing 2% zein. Both tensile and flexural tests result in maximum properties being achieved at 40% flax without the zein treatment. Impact studies for the same material show a maximum value being achieved at 30% flax and then a decrease at 40%. This is attributed to more fiber interaction as they are closer to each other at 40% than the rest of the loadings. When treated with zein, the strength of the composite both in tensile and flexural increased, while the impact strength decreased. This is due to the fact that the failure is switching to fiber fracture instead of fiber pullout of matrix fracture and that type of failure has lower energy dissipation. DMA showed that both the storage and loss modulus are increased with the addition of fibers and zein and  $T_g$  is slightly increased with the addition of zein.

Kim<sup>28</sup> on the other hand, tried to use zein protein as a binder. Gluten (wheat protein) was the main matrix used for this study, but they also used soy protein, milk powder, and amylase. Each material, excluding amylase, was



also mixed with corn starch. Zein content was varied from 4 to 32% and samples were compression molded. Compression testing was conducted to determine the materials mechanical properties. This showed that stress increased to a maximum at a zein concentration of 22% and then steadily decreased after that. They also determined that the higher applied load during processing increased the maximum stress levels.

### **1.9. Soy Protein Film Processing and Soy Protein Composites**

Another protein that is getting some discussion as a green alternative for use in the composites industry is soy protein. It has also been pursued as a standalone polymer replacement.

Mo et al<sup>29</sup> studied the curing process of soy protein isolate (SPI) to determine what process change gives the optimal material. SPI was compression molded with varying applied loads, temperatures, and time. 25% glycerol was also added to see what effect this had on the material. DSC was conducted to study thermal properties, along with tensile testing for mechanical properties. Finally, water absorption and SEM were conducted. An applied load of 20 MPa resulted in the maximum stress and Young's modulus to occur during tensile testing and any load after that had a slight decrease in these values. Water absorption was decreased from 127 to 44% as the load increased to 20 MPa. Time was varied from 3 to 15 minutes and temperature was from 100 to 160 °C. Both of these parameters were intertwined with each other, that is at lower temperatures more time was needed for SPI to achieve optimal mechanical properties and water uptake values. As the temperature was increased, the time required decreased, but as it approached 160 °C some decomposition started to occur. An ideal temperature and time of 150 °C and 3 minutes, respectively, were ultimately chosen. The addition of the glycerol had similar results but maximum stress occurred at 140 °C instead 150 °C.

Paetau et al<sup>30</sup> similarly determined what effect starting moisture and mold temperature had on the mechanical properties and water absorption of the material. They also determined what effect different acid treatments (i.e. HCl, propionic acid, sulfuric acid, and acetic acid) had on the soy. SPI and soy protein concentrate (SPC) were used in this study with moisture levels varying from 7.1 to 16.9% and 5 to 15%, respectively. Each material was also molded at temperatures of 80 to 160 °C for SPI and 100 to 160 °C for SPC. Tensile testing for SPI showed that as moisture increased, strength increased with a maximum value at 12.5% water, but the modulus decreased as water content increased. Water absorption decreased as starting moisture levels increased, which is thought to be due to a more porous material being obtained when moisture levels are low. Increasing temperature achieved a maximum strength at 140 °C and the modulus increased slightly over the whole range. The temperature increase also caused the water absorption to decrease drastically from 165 to 80%. The SPC achieved maximum strength at 7.4% water and again the modulus decreased over the whole range. The temperature study showed a maximum strength at 160 °C with little effect on the modulus. Water absorption for the concentrate was again decreased with increasing initial moisture content and increasing temperature. Acid treatments had little effect on the mechanical properties, but decreased the water absorption by over half for the SPI and just about half for the concentrate.

Chabba and Netravali<sup>31</sup> have looked at modifying soy protein concentrate (SPC) with flax fabric and glutaraldehyde (GA). SPC resin sheets were initially made with GA content ranging from 5 to 50% and also with glycerin ranging from 10 to 20% to determine the optimal amount of each. Tensile testing showed that 40% GA and 10% glycerin was optimal. TGA of the resin sheets showed that the introduction of GA improved the materials thermal

stability. DMA also showed an increase in  $T_g$  by 12 °C and an increase in storage modulus when compared to SPC alone and 10 % glycerin. Tensile testing showed that when the optimal resin was molded with flax fiber fabric, the material was better than a composite made with jute fabric and Biopol™. Also, flexural testing showed that the new composite performed as well as a composite made of cotton/kapok-polyester.

Wang et al<sup>32</sup> used cellulose whiskers from cotton linter pulp to form a composite with soy protein isolate. Whisker content was varied from 0 to 30%. DSC showed that  $T_g$  decreased until 20% whisker content, but then decreased again after this. Tan delta curves from DMA also showed a similar trend as the DSC. Water absorption tests showed that uptake leveled off for all samples after 185 minutes and as the cellulose content increased, the rate of uptake decreased. Also the total amount of water absorbed was reduced with increasing whisker amount. Finally, tensile testing was conducted with the material at two different levels of relative humidity (RH) (0 and 43%). The higher RH reduced both strength and modulus, as water has a plasticizing effect on soy protein. Also, the strength reached a maximum value at 20% and decreased thereafter. The modulus continually increased, while the elongation to break constantly decreased over the whole cellulose range.

#### **1.10. Purpose for This Research**

Previous methods for extraction of corn oil and zein protein from different sources were discussed in this chapter. Rheology of zein solutions and cellulose solutions were also evaluated. Finally, literature on composite materials produced with DDGS and zein have been presented. All this previous work has provided a solid base of knowledge on the industrial uses of DDGS. However, current research on corn oil and zein extractions is primarily based on corn gluten meal (CGM) and corn gluten feed (CGF). Extraction of the oil

and zein from DDGS is rarely studied. On-site extraction of oil and zein from DDGS after the ethanol production process would not only lower the costs of the oil and zein but also create two additional products that help reduce running costs of an ethanol plant. As shown in Figure 1.6, three main products can be derived from DDGS and each of them can find important uses in different application areas. Widespread application of the DDGS-based products can add significant value to corn.

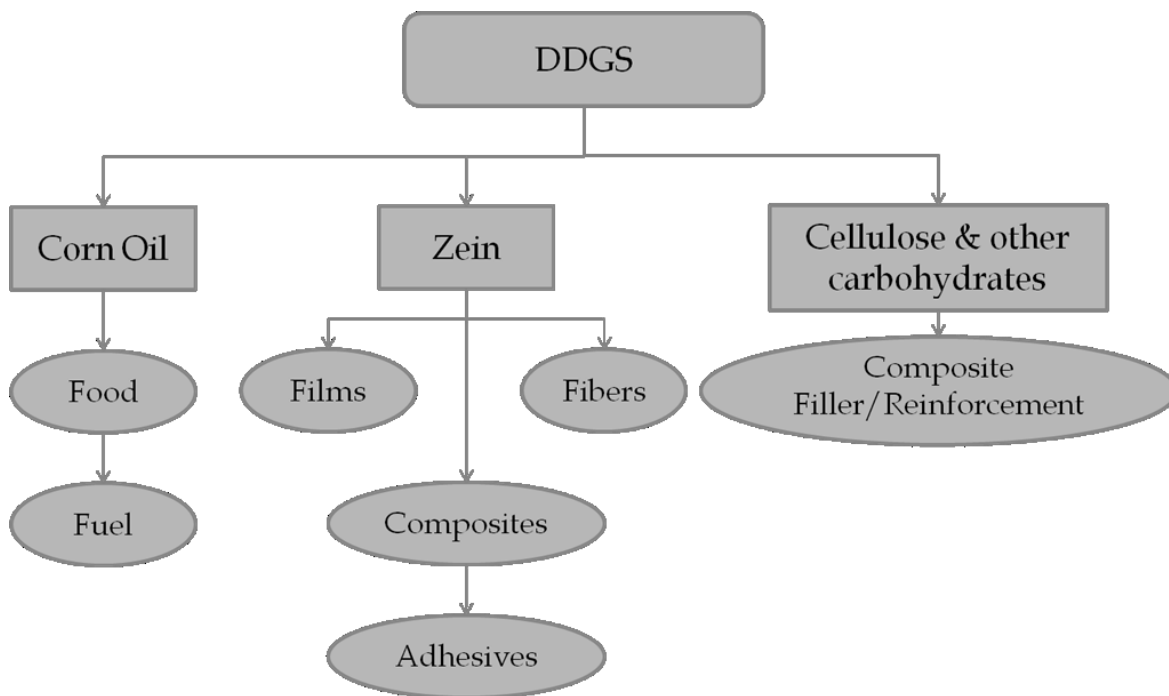


Figure 1.6. Main products derived from DDGS and their potential uses.

Nevertheless, much research has to be done before the potential of DDGS can be fully developed. Zein extracted from corn gluten meal was used as a binder material in making biobased composites. However, zein extracted from DDGS using ethanol has not been attempted as a composite material. Different extraction sources and conditions can cause large variations in zein molecular weight and properties. Studies need to be conducted to determine

the suitability of the DDGS-derived zein as a composite material and the properties of the resulting composites.

Using zein protein as an adhesive has been studied only minimally during the initial fascination with zein as an alternative material. Zein as an adhesive shows inferior performance compared to other commodity adhesives such as epoxy and cyanoacrylate (super glue). The introduction of additives and reinforcements to zein is expected to improve its performance and make zein adhesive a commercially viable alternative to current retail adhesives. To achieve a better understanding of how to improve the adhesive the rheological and adhesion properties of zein adhesive samples with various formulations (chemical agents and reinforcement) needs to be determined.

DDGS residual after oil and zein extraction comprise mainly cellulose and other carbohydrates. Cellulose is widely used as a filler or reinforcement material in composite manufacturing. Therefore the DDGS residual has high potential to be used as a composite material and research needs to be carried out to explore it.

As such, the overall goal of this thesis is to maximize industrial utilization of DDGS via developing zein and the DDGS residual into adhesive and composite materials. Four specific objectives to achieve the overall goal include:

1. Optimize extraction condition for corn oil and zein from DDGS
2. Develop zein protein based adhesive
  - a. Rheological studies
  - b. Adhesion studies
3. Develop and optimize soy/zein composites
4. Develop DDGS/zein composites

The focus of this thesis will be on objectives 2, 3, and 4. Objective 1 is a necessary preparation for the rest three objectives. In addition, successful completion of this objective will prove that on-site extraction of oil and zein from DDGS in a corn ethanol plant is feasible. The results from objective 1 are presented in Appendix 1 due to its relatively short length.

## **CHAPTER 2. RHEOLOGY OF ZEIN PROTEIN AND ZEIN/CELLULOSE NANOFIBRILS SOLUTIONS AND ITS USE AS A WOOD ADHESIVE**

### **2.1. Introduction**

Previous rheological studies have shown that additives<sup>20</sup> and varying pH values<sup>21</sup> can change the characteristics of zein solutions. Zein has also previously been shown that it can function as an adhesive with satisfactory results.<sup>19</sup>

To use a zein solution as an adhesive an understanding of its flow characteristics is needed. This can be achieved by conducting rheology measurements. Also the introduction of cellulose nanofibrils (CNF) into zein solutions could not only help improve mechanical properties but it could also help tailor the viscoelasticity of the adhesive which is important in practical applications.

The overall objective of this part of the research was to determine the rheological properties of zein solutions and zein solution/CNF mixtures. Followed by taking some of these solutions and mixtures and use them as a wood adhesive. Performance of these adhesives will be determined by shear testing of a lap joint.

### **2.2. Materials and Methods**

#### **2.2.1. Materials**

CNF in a gel form (1.8% CNF/water dispersion) was obtained from USDA Forest Products Laboratory. Twisted/untwisted, curled/straight, and entangled/separated cellulose nano-fibrils ranging from 5 to 100 nm in diameter can be identified from Figure 2.1. Several large fibers were actually bundles of small fibrils. The highly entangled structure of CNF significantly increased its resistance to flow and was attributed to the gel-like behavior of the as-received CNF gel sample.

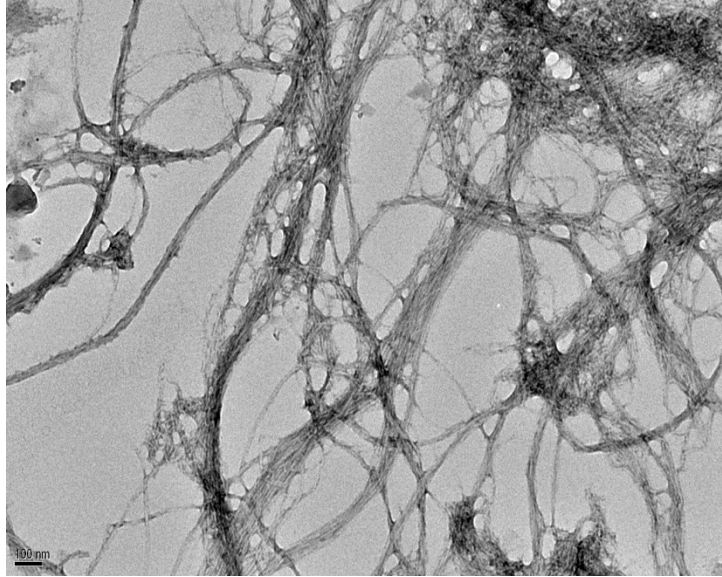


Figure 2.1. A TEM image showing networks of CNF.

Corn zein (F-4000) was obtained from Freeman Industries (Tuckahoe, NY). Glutaraldehyde (GA) was purchased from Fisher (Pittsburgh, PA). Titebond® original wood glue (aliphatic resin) (Columbus, OH).

### **2.2.2. Processing**

#### **2.2.2.1. Zein Solutions**

Solutions containing 1, 3, 5, 7, 9, 13, 15, 20, and 25% zein protein were prepared in an 80% aqueous ethanol solvent. These were then used for rheology testing and the three highest percentages were used for a wood adhesive. Those three were also combined with 3% GA, (based on dry weight of the zein), to evaluate the effects of the GA crosslinker on the adhesion properties.

#### **2.2.2.2. Zein/CNF Mixtures**

The CNF and zein mixtures were made by adding various amounts of CNF gel to the three highest zein solutions plus an additional 11% zein solution. CNF concentrations were held to 1, 0.8, and 0.6% based on total weight. When the top three pure zein concentrations and the 11% zein concentration were



added to the 1% CNF this resulted in zein concentrations of 11, 9, 7, and 5%, respectively. When they were added to the 0.8% CNF mixture this resulted in zein concentrations of 14, 11, and 8% zein for the top three and 6% zein for the 11% solution. Finally when the top three zein concentrations were added to the 0.6% CNF this resulted in 17, 13 and 10% zein and 7% zein for the 11% solution.

To prepare samples for adhesive strength testing, the mixtures were applied to the surface of two wood bars, which are shown in Figure 2.2. A jig, as seen in Figure 2.3, was constructed to hold the two bars together as the adhesive was allowed to dry. It consisted of two steel plates with aligned holes for bolts to go through that would compress the bars. Four pairs of bars could be put in one jig, which provided repeats for consistency. An area of 12.7 x 25.4 mm was used for adhesive application on the wood bars. Samples were dried in a vacuum oven at 65 °C and 380 mmHg for at least 14 hours. After removal from the oven each sample was tested for tensile properties.



Figure 2.2. Wood bars used for adhesive lap-shear testing.



Figure 2.3. The compressive jig used to make zein adhesive samples.

### **2.2.3. Rheological Testing**

Rheological testing was conducted on a TA AR-G2. Steady shear tests were conducted over a shear rate range of 0.1 to 100 1/s at a temperature of 25 °C. Dynamic shear testing first needs to have a shear strain determined that is in the linear elastic region. This was achieved by conducting strain sweeps with a range of 0.1 to 100% strain, a frequency of 1 Hz and a temperature of 25 °C. This was then followed by frequency sweeps with a range of 0.04 to 100 rad/s and 25 °C and at the corresponding shear strain determined previously.

### **2.2.4. Mechanical Testing**

Lap shear testing was conducted on the adhesive samples following a modified ASTM D1002. Specimens consisted of two 25.7 x 108 mm wood blanks and an overlap area of 12.7 mm. An Instron tester (5567) equipped with a 30 KN load cell was used with a testing speed of 1.3 mm/min. Testing was repeated four times for consistency. The calculated strengths are determined using the maximum average load from tensile testing and the area of overlap. Modulus was calculated by determining the slope of the linear region of the stress-strain curves.

### **2.2.1. Microscopy**

Images of the adhesive fracture surfaces were captured using a JOEL (JSM-6490LV) scanning electron microscope (SEM) operating at 10Kv. Sample surfaces were sputter coated with gold before the tests.

## **2.3. Results and Discussion**

### **2.3.1. Rheology Results**

#### **2.3.1.1. Steady Flow Results**

Representative curves of steady shear viscosities of the pure zein solutions with different zein concentrations were compared in Figure 2.4. As a general trend, the viscosity increased with zein concentration because larger contents of zein in the solutions caused higher resistance to the flow of the solutions. All the solutions showed shear thinning behavior, i.e. their viscosities decreased with increasing shear rate. This was due to the alignment of zein molecules in the direction of flow, which reduced their resistance to the flow. The trend of decreasing viscosity with increasing shear rate matches data collected by Zhang et al <sup>21</sup>. Figure 2.4 also shows that the shear thinning behavior was more severe at higher zein concentrations, i.e., the slopes of the curves at low shear rates ( $< 1 \text{ S}^{-1}$ ) increased with zein concentration. This was due to the increasing contribution from zein to the flow behavior of the solutions.

The addition of CNF increased solution viscosities substantially. These values are seen in Figures 2.5 thru 2.7, which show the results for a pure zein solution and zein solutions containing CNF. By comparing the three charts, it is obvious that as CNF content increased so did the mixtures viscosity, while the zein concentration had little effect on viscosity. This observation indicates that CNF dominated the rheological behavior of the mixtures due to its entangled network structure, which imposes significant

resistance to the flow of the mixtures. These mixtures also showed a shear thinning behavior as the shear rate increased, a behavior similarly to pure zein solutions, which can be attributed to the alignment of not only the zein molecules but also the CNF fibers. The significantly increased viscosity of the mixtures is beneficial to adhesive applications of zein as it can prevent dripping of the adhesives from material surfaces. The viscosity of the adhesive can also be varied to suit different adhesive applications by a small adjustment on CNF concentration.

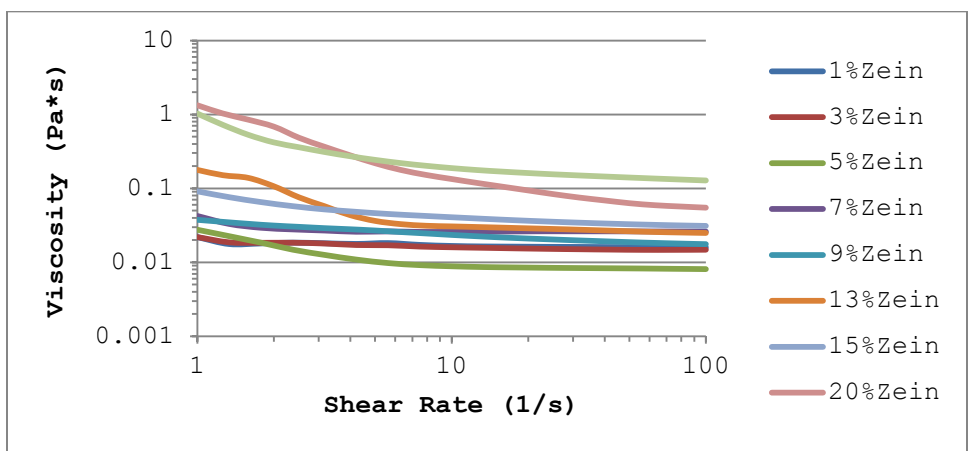


Figure 2.4. Viscosity as a function of shear rate for pure zein solutions.

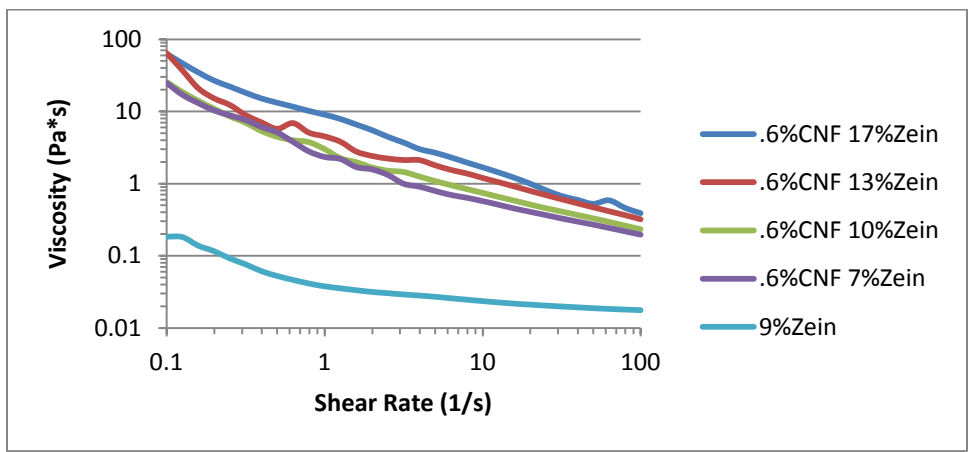


Figure 2.5. Viscosity as a function of shear rate for .6% CNF and zein mixtures.

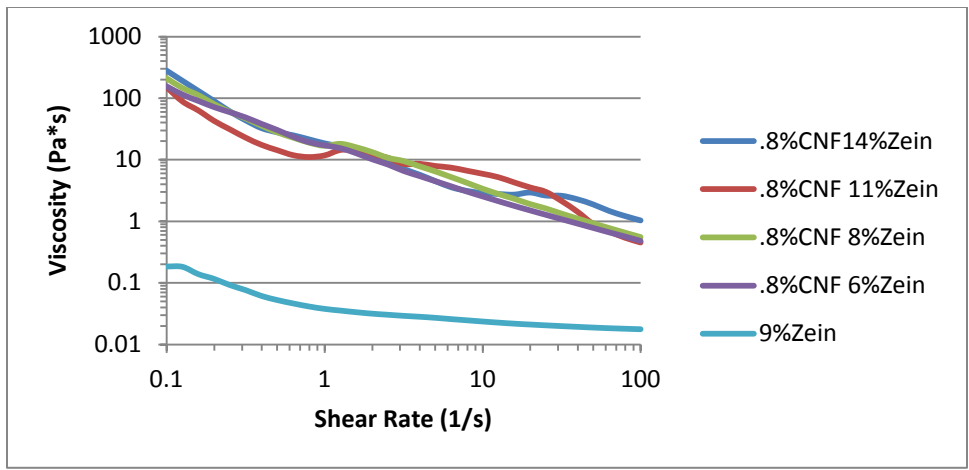


Figure 2.6. Viscosity as a function of shear rate for .8% CNF and zein mixtures.

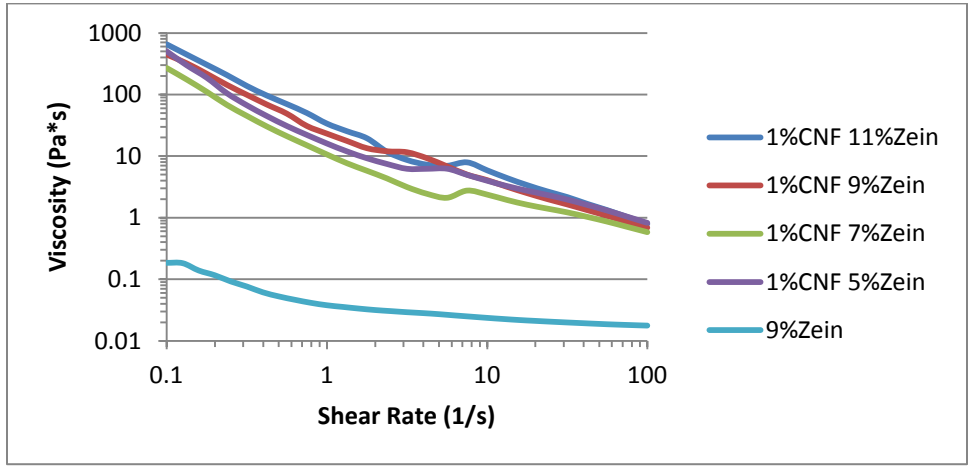


Figure 2.7. Viscosity as a function of shear rate for 1% CNF/zein mixtures.

The critical concentration or the point where the particles or fibers in a solution start to interact with each other is found by comparing the viscosity at zero shear.<sup>23</sup> The viscosity of pure zein solutions fluctuated at zero shear, so the values from the six 1/s were used instead to give a rough estimation of the critical concentration. A graph showing the results for this analysis is presented in Figure 2.8. The critical concentration for the zein solutions is at approximately 10% zein concentration.

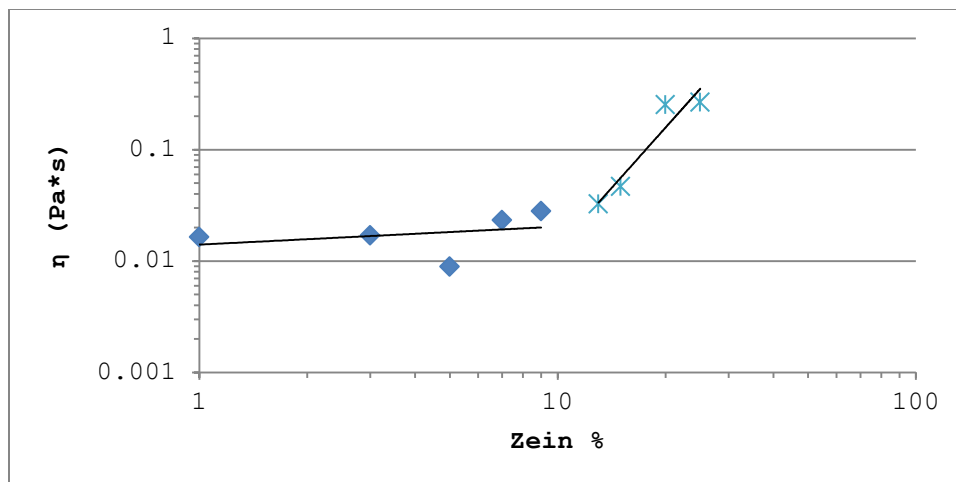


Figure 2.8. Viscosity as a function of zein concentration showing deflection at the critical concentration.

### 2.3.1.2. Dynamic Rheology Results

Frequency sweeps were also conducted for all solutions and mixtures to examine their viscoelasticity. Due to the low viscosity of the pure zein solutions, large fluctuations of values for storage ( $G'$ ) and loss ( $G''$ ) moduli were recorded and therefore the data is not shown. However, a general trend of increase in the modulus with zein concentration could still be discerned from the scattered data.

The zein/CNF mixtures with increased viscosities showed significantly reduced statistical deviation. Their storage and loss moduli are shown in Figures 2.9 and 2.10, respectively. These two figures show increases in both  $G'$  and  $G''$  as fiber content increases. These increases correspond to the increase in complex viscosity of the mixtures as shown, in Figure 2.11. It is also worth noting that in all the three figures, the properties (i.e. modulus and viscosity) increase with decreasing zein concentration, again indicating that CNF was the dominant factor in controlling the viscoelastic properties of the mixtures.

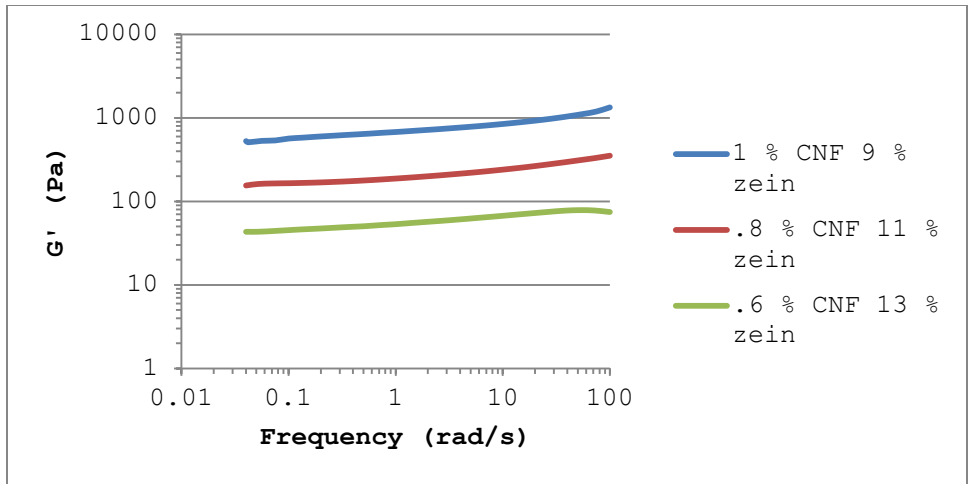


Figure 2.9. Storage modulus curves of the zein/CNF mixtures with different CNF concentrations.

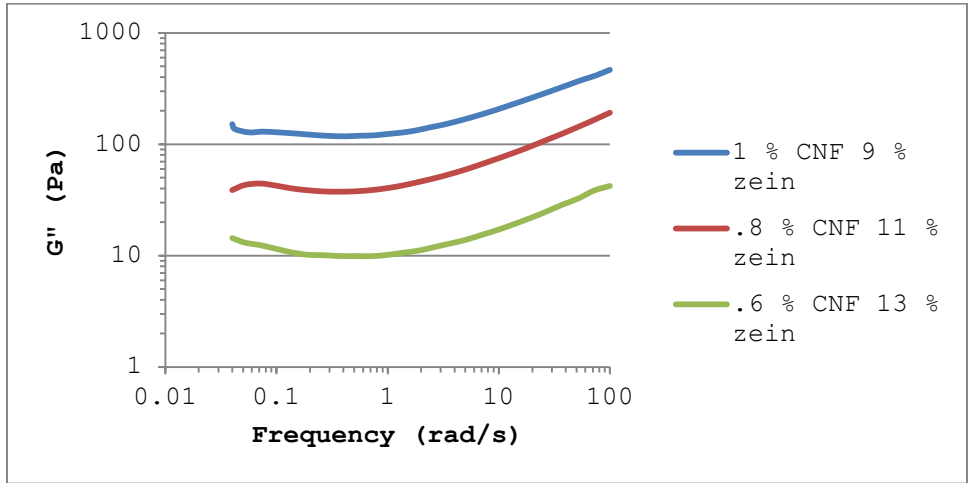


Figure 2.10. Loss modulus curves of zein/CNF mixtures with different CNF concentrations.

$G'$  and  $G''$  of the three previous mixtures are compared in Figure 2.11.  $G'$  of all the mixtures is higher than their corresponding  $G''$ , which implies that the mixtures are more elastic than viscous due to the CNF networks. By contrast, pure zein solutions are more viscous ( $G'' > G'$ ) because they lack the ability to store mechanical energy.

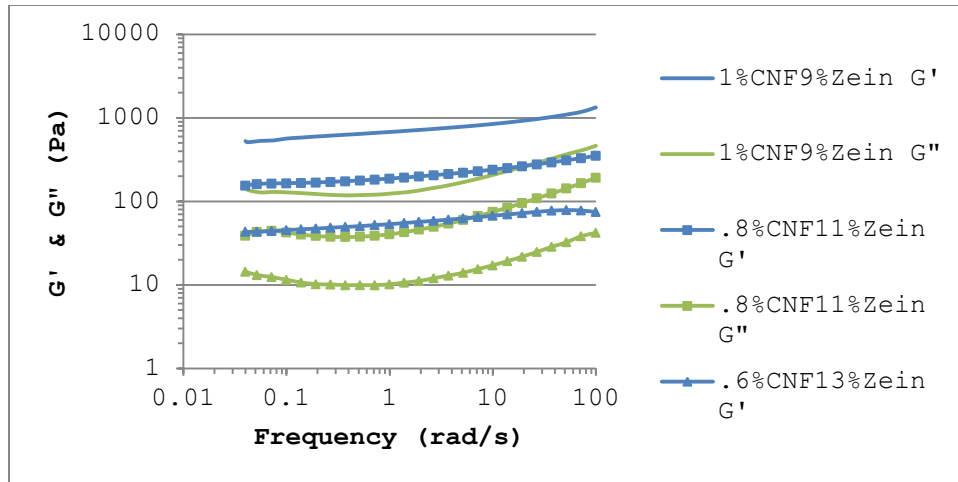


Figure 2.11.  $G'$  and  $G''$  curve comparisons of zein/CNF mixtures with different CNF concentrations.

The complex viscosity of zein/CNF mixtures are shown in Figure 2.12. The behavior of the complex viscosity is similar to that of the steady shear viscosity: decreases in viscosity with increasing frequency (rate) and increases in viscosity with increasing CNF concentration.

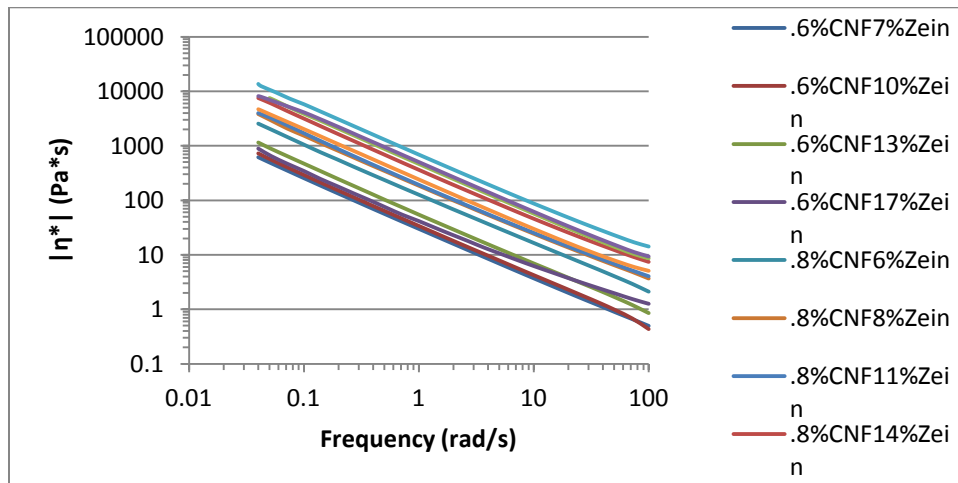


Figure 2.12. Complex viscosity of various zein/CNF mixtures.

### 2.3.2. Zein and Zein/CNF Adhesive Results

The shear testing results for zein and zein/glutaraldehyde (GA) adhesive are shown in Figure 2.13 and a picture of the wood specimens after fracture can be seen in Figure 2.14. Figure 2.13 that as zein content



increased so did the strength and modulus of the adhesive. The introduction of GA had a negative effect on the adhesion strength. GA should be able to react with amino acids of zein protein even at room temperature.<sup>34</sup> The lowered strength may be due to insufficient reaction time or GA concentration. Further research is needed to identify the accurate reasons. Retail wood glue (aliphatic resin) was tested under the same conditions for comparison. The results show that zein as an adhesive is inferior to the commercial glue.

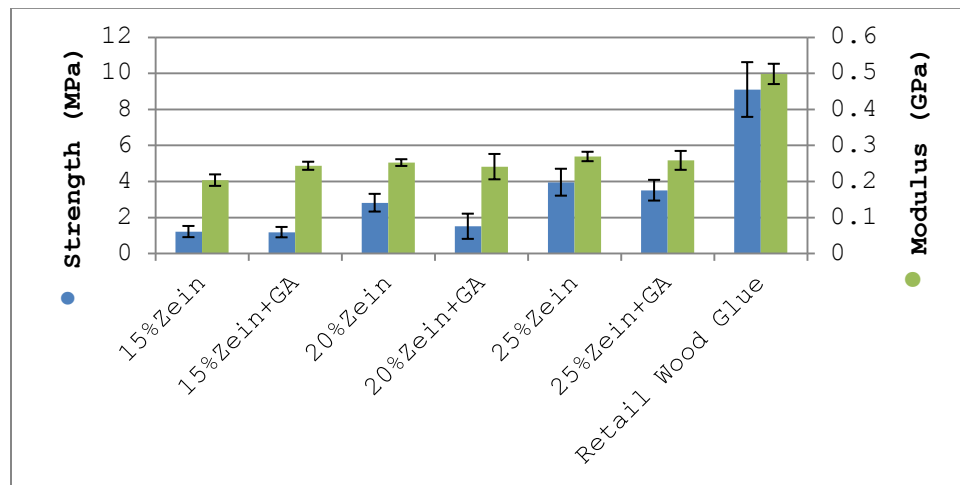


Figure 2.13. Tensile testing results of zein and zein + GA adhesives.

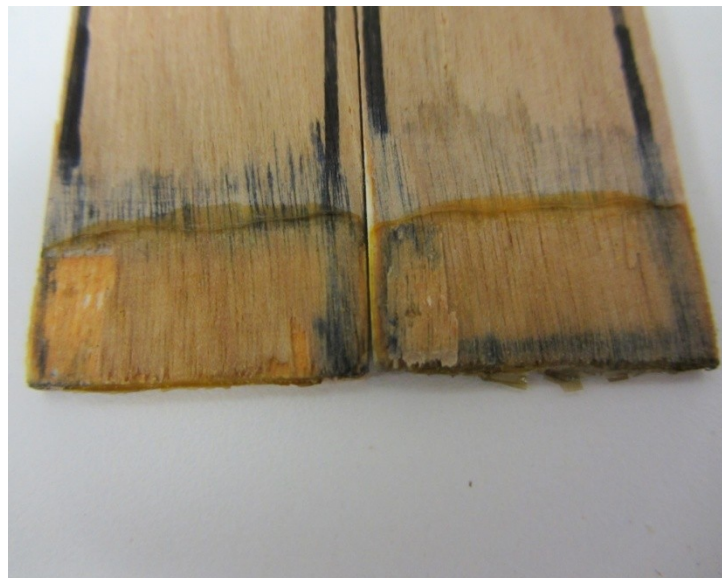


Figure 2.14. Picture of the fracture surface of a wood adhesive specimen.

CNF was added to pure zein solutions to improve the mechanical properties of the zein adhesives. Figure 2.15 compares the strength and modulus of adhesives comprised of different ratios of zein and CNF. It shows that the strength increases with both CNF and zein content but is affected more by the increase in CNF content. For instance, 1%CNF-9%Zein showed higher strength than did 0.6%CNF-17%Zein and 0.8%CNF-14%Zein. Finally for both the pure zein and zein/CNF mixture adhesives the modulus is largely unaffected by either zein or CNF content.

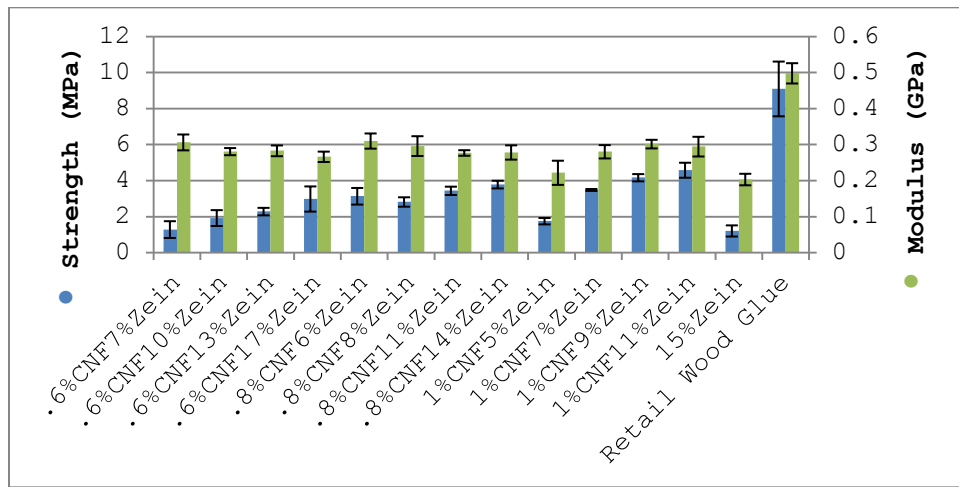


Figure 2.15. Tensile testing results for various zein/CNF adhesives.

### 2.3.3. Microscopy

The fracture surfaces of pure zein adhesive and zein/CNF adhesive were studied using SEM. Figure 2.16a present a SEM image of the wood surfaces before applying the pure zein adhesive, while b and c are the fracture surfaces of the adhesive bond. When comparing between the wood and fracture surface pictures, it is seen that the wood surface was smoothed by the adhesive coating as the particles, edges, and fibers on the wood surface are less discernible. The adhesive showed minimal plastic deformation after bond fracture as no adhesive material was pulled up from the surfaces. The fracture surfaces also show minimal damage to the wood surface after

fracture, thus indicating that the failure was primarily a cohesive failure of the adhesive.

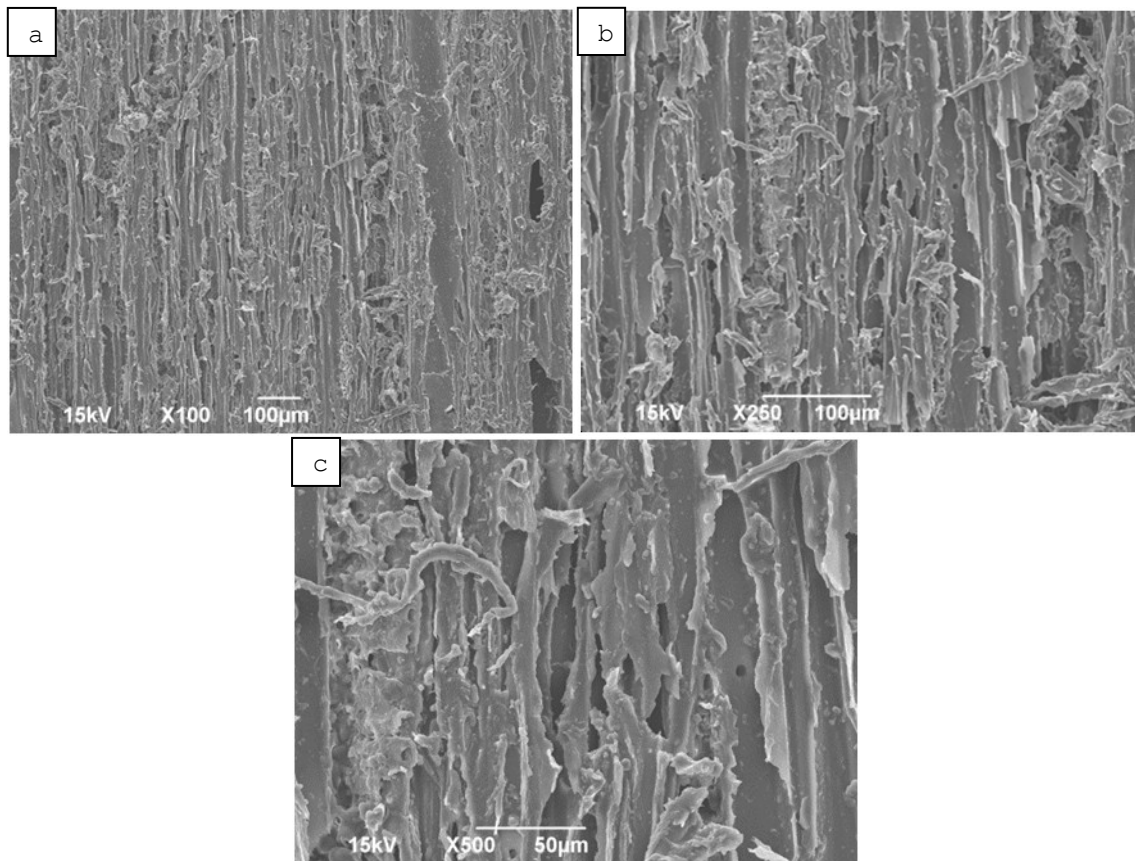


Figure 2.16. SEM images showing the wood surfaces without pure zein adhesive (a) and the fracture surfaces of the 25% pure zein adhesive bond (b and c).

Figures 2.17a-d below presents SEM images showing the fracture surfaces of the zein/CNF adhesive bonds. The pictures show a striking difference from the fracture surfaces of the pure zein bonds where wood damage is negligible. Here fibrils of the adhesive material were pulled out from the surfaces (a and b). The capability of undergoing this kind of large plastic deformation was imparted to the adhesive by the entangled network of CNF. Moreover, a better adhesion between the adhesive and wood surface was achieved after the addition of CNF to pure zein. This is evident from the wood fibers being pulled up from the surfaces (c and d), indicating a transition from adhesive

failure to cohesive failure. This enhanced adhesion could be due to mechanical interlocking between the CNF network and the porous wood surface.

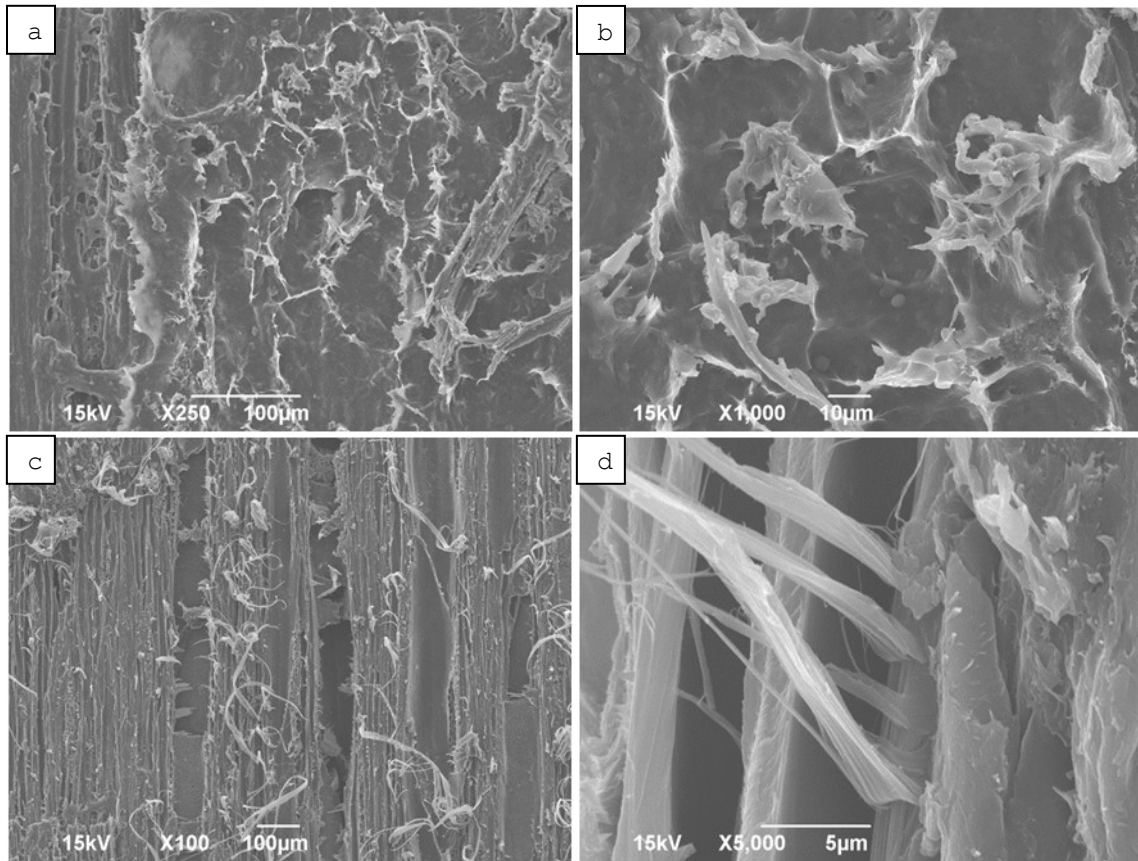


Figure 2.17. SEM images of the fracture surfaces of zein/CNF adhesive bonds. Adhesive formulation: 1% CNF and 11% Zein.

Figure 2.18 shows representative stress and strain curves for zein and zein/CNF adhesives. Here the more ductile nature for the zein and zein/CNF bond can be seen, as the two curves for the respective adhesives has a lower maximum stress but is able to achieve a higher maximum strain. This would correlate with the SEM images shown above.

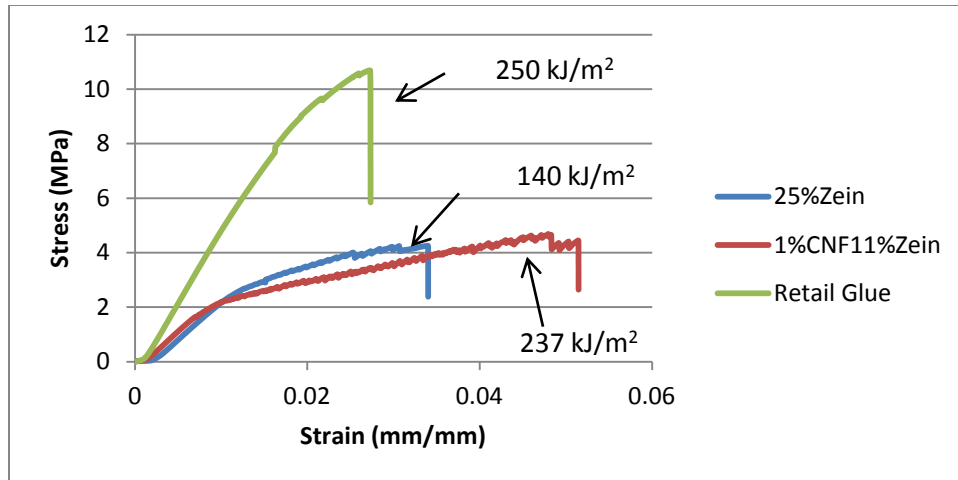


Figure 2.18. Representative stress and strain curves for zein and zein/CNF adhesives.

#### 2.4. Summary of Results

The rheological nature of zein protein solutions with varying concentrations and the addition of cellulose nano-fibers were attained. It showed that as the zein concentration increased so did the solutions viscosity. A critical concentration was determined to be around 10% zein protein.

Rheological data for the zein/CNF mixtures showed a highly viscous material. The steady flow data showed that the viscosity of the mixtures increased with CNF concentration and the effects of CNF concentration outweighed the contribution provided by the zein concentration to the viscosity of the materials. The dynamic shear data showed that  $G'$  and  $G''$  of the mixtures also increased with CNF concentration.  $G'$  was found to be higher than  $G''$  over the whole experimental frequency range for all the mixtures. This indicates that the addition of CNF to the zein solutions transformed them from a viscous material into a more elastic material.

Finally the zein and zein/CNF solutions were used as a wood adhesive. It was shown that the pure zein protein solution is able to adhere wood but

not on comparable levels with current retail wood glues. A maximum of 4 MPa was achieved with the 25% zein protein solution. The addition of GA to the solutions decreased the properties of the zein adhesive, which is worth further research. On the other hand the addition of CNF to the zein solutions caused a large increase in tensile strength and fracture toughness. The SEM images show that the CNF was able to attain a better mechanical interlock with the wood surface. This research on the rheological properties of the zein and zein/CNF solutions and the use of zein as an adhesive in conjunction with CNF have shown that zein adhesives with CNF can be a viable replacement for current wood glues. Further research on formulation and process is required to improve the performance of the zein adhesive.

## CHAPTER 3. SOY PROTEIN AND ZEIN PROTEIN COMPOSITES

### 3.1. Introduction

Zein is capable of modifying fibers in composites to improve compatibility between the two materials<sup>27</sup> and also as standalone binder to create a composite of just zein and another material.<sup>28</sup> Also zein has been shown to combine with soy protein isolate to form a composite material.<sup>28</sup>

The objective of this portion of the research was to understand the performance of DDGS-derived zein as a constituent material in composites. Soy and zein protein were combined to produce a composite material via compression molding. Plasticizers and crosslinkers were also added to investigate their effects on the composite characteristics. The samples were then tested for mechanical, thermal properties, and morphology using compression testing, thermogravimetric analysis (TGA) and microscopy.

### 3.2. Materials and Methods

#### 3.2.1. Materials

Poly(ethylene glycol) (PEG) MW 400 and Poly (propylene glycol) (PPG) MW 400 were obtained from Alfa Aesar (Ward Hill, MA). Glycerol was obtained from Mallinckrodt Chemicals (Phillipsburg, NJ). Corn zein (F-4000) was obtained from Freeman Industries (Tuckahoe, NY). Soy protein isolate (SPI, Profam 974) powder was obtained from Archer Daniels Midland Company (Decatur, IL). Glutaraldehyde (GA) 50% was purchased from Fisher (Pittsburgh, PA).

#### 3.2.2. Processing

A certain amount of zein was dissolved in 80% aqueous ethyl alcohol on a stirring plate. After the zein had completely dissolved predetermined contents of the SPI were added to achieve SPI/zein ratios of 90/10 and 85/15. The mixtures were mechanically stirred to allow uniform SPI dispersion. Enough absolute ethanol was subsequently added to the mixtures to increase

the ethanol concentration to over 95%. The dissolved zein precipitated out from the solution under this ethanol concentration and coated the SPI powder. With the excess ethanol decanted off any additives were then added to the damp material. All plasticizers (i.e. PEG, PPG, glycerol, and glycerol/PPG (1:3)) were added at 20% based on total dry weight of the proteins (i.e. zein plus soy protein) and the crosslinker glutaraldehyde (GA) was added at 3% of the total dry weight. The mixture was manually stirred for uniform dispersion and was then placed in a compression mold for processing. A hydraulic press was used to apply load and heat on the mold. After compression the sample was removed from the mold and conditioned at ambient temperature for 24 hours prior to tests.

The compression molding was performed at both room and elevated temperatures. For the later, temperatures of 160 °C for the top platen and 120°C for the bottom platen were adopted due to unbalanced heat conduction of the mold. The center of the mold was measured to have a temperature of approximately 130 °C. The mold was then placed in the hot press for 30 minutes and allowed to heat up. A load of 9.5 tons was applied to the mold for 30 minutes. At room temperature a load of 2 tons was applied.

### **3.2.3. Mechanical Testing**

Compression testing was used to study the mechanical properties of the samples. A modified ASTM standard D695 was followed for this testing. Specimens were 12.7 x 18.5 mm. The compression tests were conducted on an Instron tester (5567) equipped with a 2 and 30 KN load cell for room and elevated temperature testing, respectively. A test speed of 1.3 mm/min was chosen for the tests. Three repeats were conducted for consistency. Strength was calculated using the cross-sectional area and the largest load obtained.



Modulus was calculated using the stress-strain graphs and calculating the slope of the linear region.

#### **3.2.4. Thermal Testing**

Thermogravimetric analysis (TGA) was performed using a TA TGA-Q500 with provided TA software. The tests were started at room temperature and ramped to 700 °C at a heating rate of 20 °C/min. Nitrogen flow (60 ml/min) was provided during the testing.

#### **3.2.5. Microscopy**

Images of fracture surfaces were captured using a scanning electron microscope (SEM) from JOEL (JSM-6490LV). The operating voltage of the SEM was 10 KV. Sample surfaces were sputter coated with gold before the tests.

#### **3.2.6. Water Absorption**

Rectangular pieces of the compression molded material (13.5x7 mm) were dried for at least 24 hours and then immersed in water over a 36 hour period. The samples were removed at 5, 10, 15, 30, 60, 120, 240, 480, 960, 1440, and finally at 1920 minutes to measure their mass.

### **3.3. Results and Discussion**

#### **3.3.1. Compression Test Results**

The material that was pressed at room temperature came out as a white, porous, and brittle material and was insufficient for tensile testing. Surface cracks were evident on some samples due to the lack of strong adhesion between the soy protein particles (Figure 3.1). Thus compression testing was used to compare mechanical properties of each sample.



Figure 3.1. SPI/zein composite obtained from compression molding at room temperature.

The compressive strength and Young's modulus of samples with different formulations are compared in Figures 3.2 and 3.3, respectively. The addition of the plasticizers or combinations of plasticizers, which were intended to improve the toughness and processability of the SPI/zein composites, did reduce the modulus of the composites. However, the modulus reducing effects of the plasticizers were different on the 90/10 and 85/15 composites. For the 90/10 composite, Figure 3.3 shows that PPG resulted in the largest modulus reduction followed by PEG, glycerol/PPG mixture and glycerol. For the 85/15 composite, glycerol/GA led to the largest modulus reduction and the glycerol still caused the least reduction. It might be due to insufficient temperature and GA concentration. Further study is required to find the reason behind this observation. It could be due to preferential distribution of the plasticizers in the SPI or zein phases of the composites. For the compressive strength, the plasticizers either reduced the values moderately or showed only negligible effects (Figure 3.2). The largely maintained strength allows

the composites to be used in the applications that require relatively high material strength.

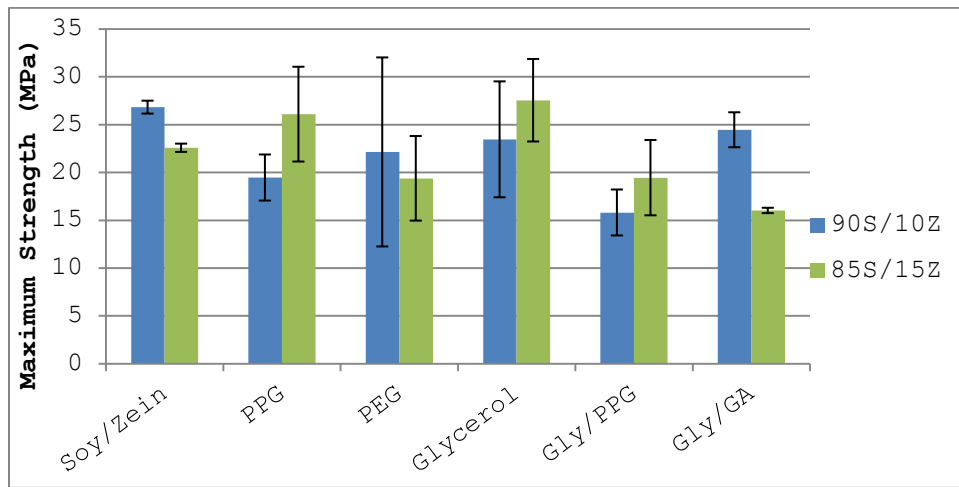


Figure 3.2. Compressive strength for samples made at room temperature. SPI/zein ratio: 90/10 and 85/15.

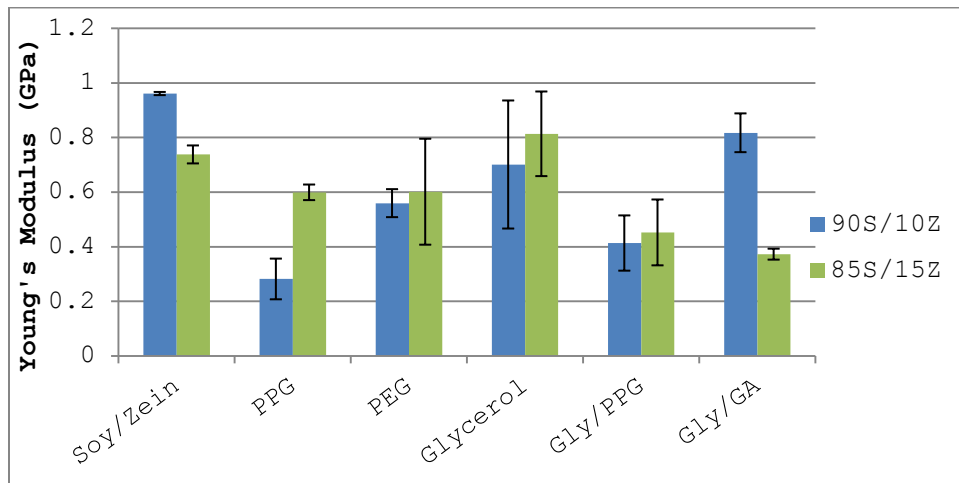


Figure 3.3. Modulus for samples made at room temperature SPI/zein ratio: 90/10 and 85/15.

When heat was applied to the materials during the compression molding, the proteins, with the assistance of plasticizers, heat, and pressure transitioned from solid powders into a plastic melt. The melt solidified inside the mold under pressure when it cooled down. A sample prepared by this process is shown in Figure 3.4. The sample was solid and smooth and had a

distinctive plastic like appearance. The compressive strength and modulus of the samples are shown in Figures 3.5 and 3.6, respectively. This process increased the mechanical properties of the material by almost doubling strength and modulus over the material produced at room temperature. This is mainly due to the better consolidation and fusion of the protein particles. PPG plasticizer significantly decreased the strength of the composites. PEG, glycerol/PPG and glycerol showed relatively small effects on the composites strength. The introduction of the crosslinker glutaraldehyde (GA) substantially improved the strength of the 85/15 composite but had little effect on the 90/10 composite, which could indicate that the crosslinking reaction mainly occurred in the zein phase. When using both GA and glycerol the strength increase caused by the crosslinker was largely offset by the plasticizing effect of the glycerol.



Figure 3.4. Soy/zein protein composite compressed at 130 °C.

As for the moduli of the composites, the plasticizers and the crosslinker showed a much weaker influence on them compared to the strength. The composite with the crosslinker showed the highest modulus. The high

standard deviation during compression testing of both the room temperature and elevated temperature samples may be due to the nature of how they are created. This method may introduce large amounts of error into these tests.

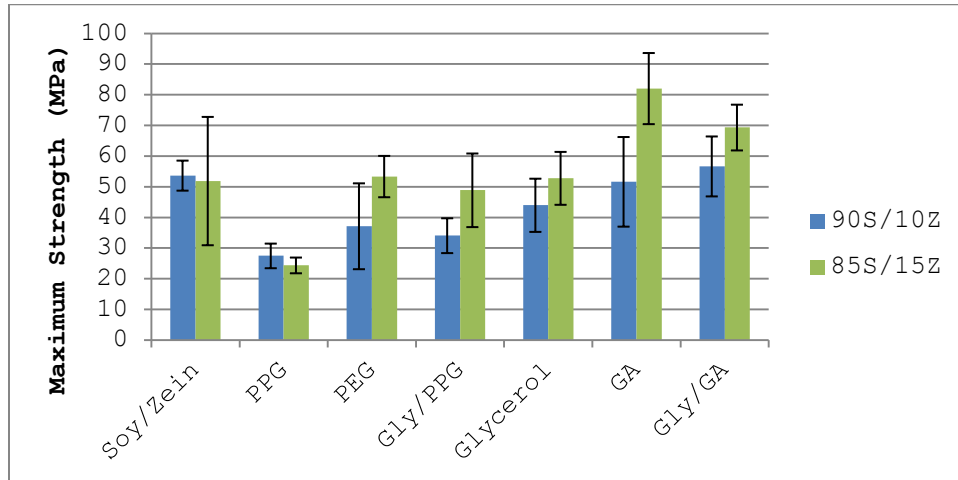


Figure 3.5. Compressive strength of the composites compressed at 130 °C.

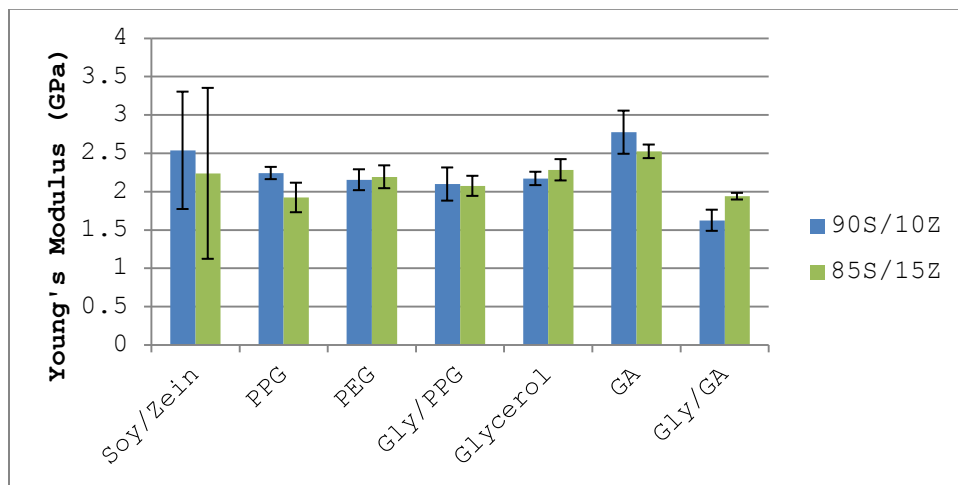


Figure 3.6. Modulus of the composites compressed at 130 °C.

Representative stress and strain curves are presented in Figure 3.7, along with estimated toughness values for each curve. Here it can be seen that the introduction of GA to the soy/zein material increases overall strength and toughness. When glycerol is added along with GA an improvement over straight plasticizer is still attained but maximum strength is reduced.

Even with a reduced strength the sample comprising of plasticizer and crosslinker achieved a larger toughness value.

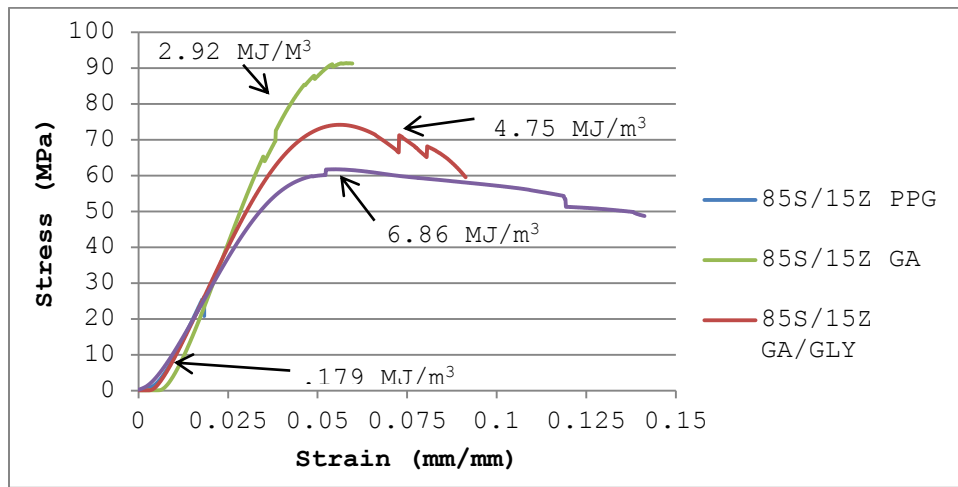


Figure 3.7. Stress-strain curves of selected composites with fracture toughness indicated on the curves.

### 3.3.2. Thermogravimetric Analysis

Thermal stability of the composites was investigated using TGA. The results are assembled in Table 4.1 with values for initial degradation temperature (IDT), percent weight loss over the largest loss region, and residual weight percents from the end of the tests. Figure 4.8 shows the TGA and dTGA curves for all samples. The TGA curves for all of the samples were pretty similar showing that the plasticizers had little effect on the thermal stability of the composites. The dTGA curves do show though that both samples containing PEG had a higher weight loss rate than the rest, except for the 85/15 sample that had a higher rate than even the PEG sample. Table 1 also shows that the composites containing GA crosslinker have the highest residual weight, indicating that the thermal resistance of the proteins was improved after crosslinking.

Table 3.1: TGA Results for Initial Degradation Temperature (IDT), Percent Weight Loss, and Residual Weight of SPI/Zein Composites.

Sample ID	IDT (°C)	Weight Loss (%)	Residual Weight
90S/10Z	248	61.1	12.07
90S/10Z PEG	240	67.1	12.17
90S/10Z GLY	160	70.4	11.87
90S/10Z GA	250	61.8	16.35
85S/15Z	256	64.3	11.96
85S/15Z PEG	230	68.3	12.05
85S/15Z GLY	182	66	10.57
85S/15Z GA	253	59	16.35

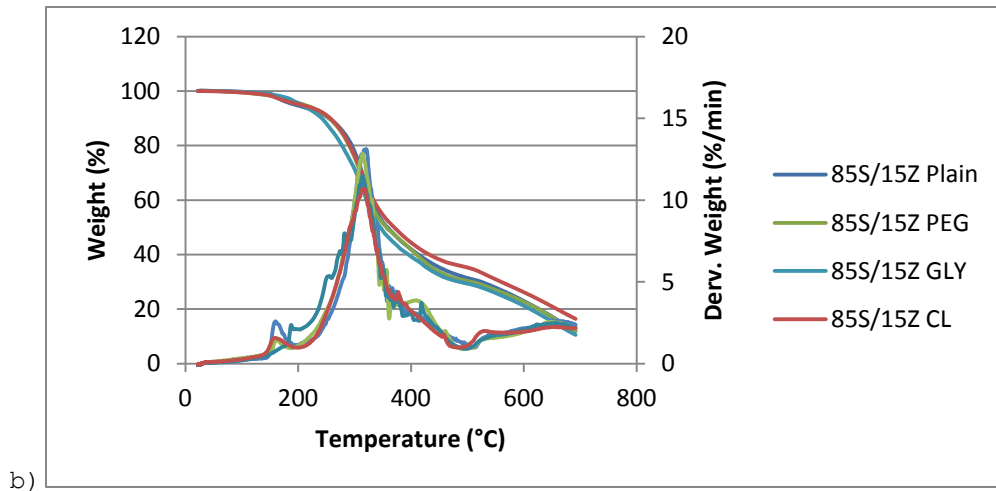
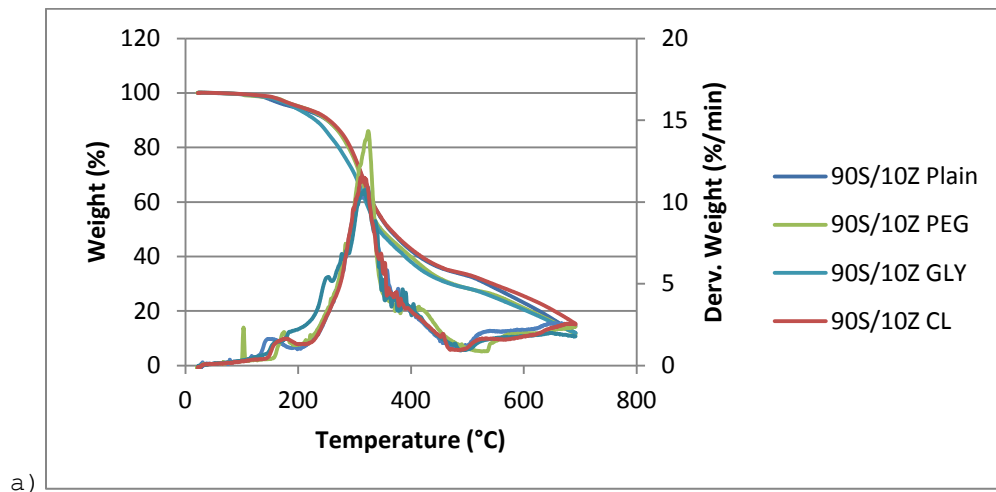


Figure 3.8. TGA and dTGA curves for a) 90/10 b) 85/15 ratio samples.

The values for IDT are in line with values reported by Schmidt et al<sup>35</sup> on SPI and Sodium dodecyl sulfate (SDS), which were in the range from 260 °C to 290 °C. Otaigbe et al<sup>36</sup> and Chen et al<sup>37</sup> also had TGA curves that showed IDT for SPI materials from 200 °C to 260 °C.

### 3.3.3. Microscopy

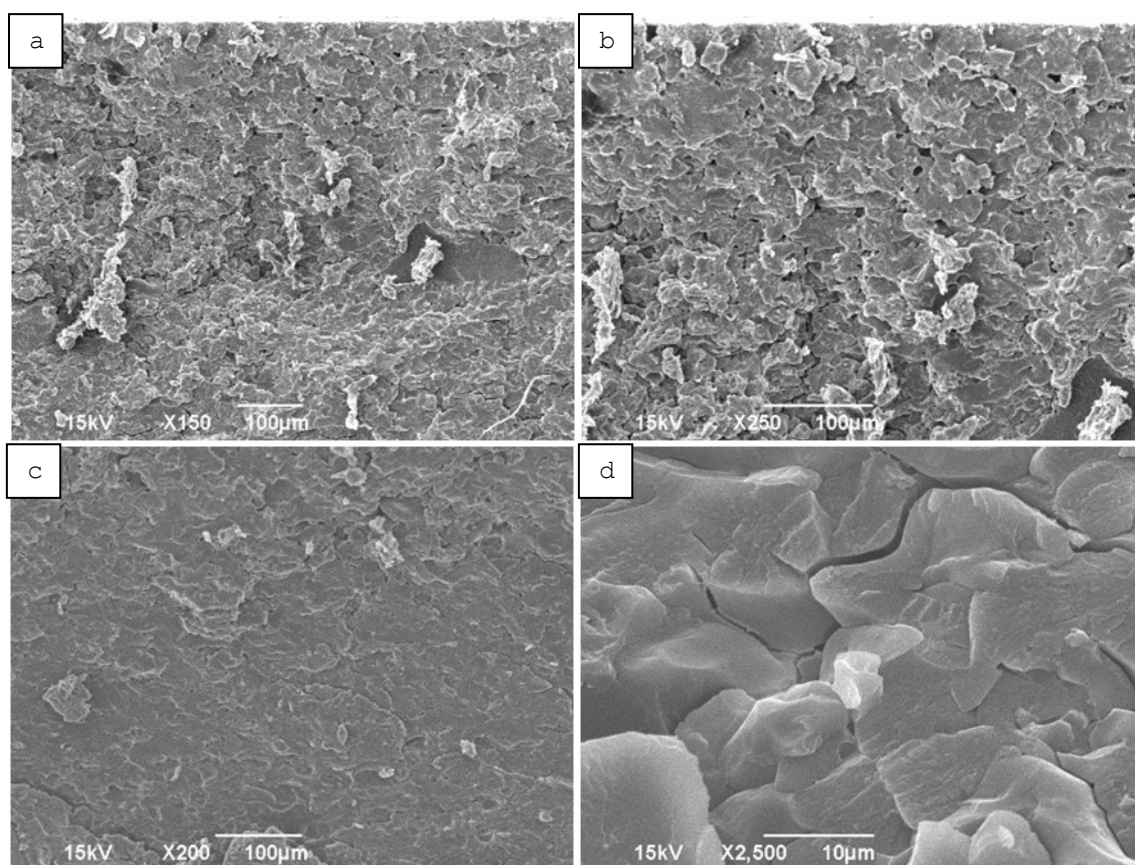


Figure 3.9. SEM images showing morphological differences seen in 85/15 sample.

Some samples molded with heat showed non-uniform morphology. The color of some parts of the sample (mostly on the surface) appeared lighter compared to the rest of the sample. SEM micrographs show that in these areas a complete protein plasticization and consolidation is lacking and the sample contains many micro-sized void (Figures 3.9a and b). By contrast, the areas that appeared darker exhibit full consolidation without discernible voids (



Figures 3.9c and d). The morphology of the lighter parts resembles that of the samples molded at room temperature. The voids embedded in these parts are detrimental to mechanical properties of the samples. Improvements in processing conditions including balanced heat transfer and optimized dwell time and compression pressure can be used to increase sample quality.

### 3.4. Water Absorption Testing

Curves showing the water absorption trends for the elevated heat compression molded SPI/zein composites are presented in Figure 3.10. All samples had high absorption rates during the first 2 hours of the testing. All 90/10 samples showed slightly lower overall water absorption compared to 85/15 samples. The samples without any additives (i.e. 85S/15Z and 90S.10Z in the figure) showed the highest water uptakes. The addition of the plasticizers or crosslinkers decreased the absorption. A synergy was observed when the plasticizers and crosslinkers were used together. This synergy is attributed to the improved plasticization and consolidation of the proteins with the assistance of the plasticizers and the chemical reaction incurred by the crosslinker.

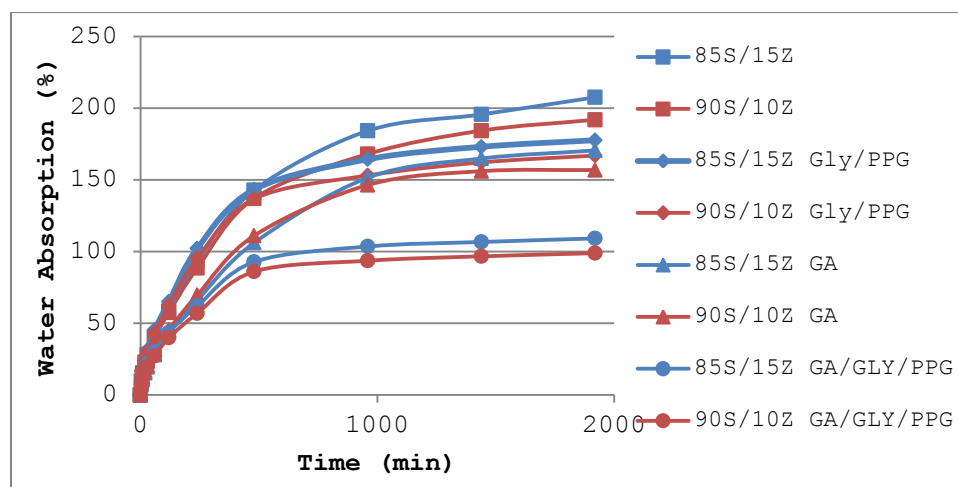


Figure 3.10. The water absorption of compression molded soy/zein protein samples.

Apparent diffusion coefficients ( $D_A$ ) can be calculated following the equation provided by Anderson.<sup>38</sup>

$$D_A = \pi * \left[ \frac{h}{4 * M_{sat}} \right]^2 \left[ \frac{\partial M_t}{\partial \sqrt{t}} \right]^2$$

This equation takes into account the thickness of the sample ( $h$ ), the moisture uptake at saturation ( $M_{sat}$ ), and the slope of the moisture uptake versus the square root of time ( $\frac{\partial M_t}{\partial \sqrt{t}}$ ). Values obtained from substituting the appropriate values into this equation are shown in Table 3.2.

Table 3.2: Apparent Diffusion Coefficient ( $D_A$ ) Values for Soy/Zein Samples.

Sample ID	$D_A$ (mm <sup>2</sup> /min)
85S/15Z GLY/PPG	0.00241
85S/15Z GA	0.00131
85S/15Z GA/GLY/PPG	0.00218
90S/10Z GLY/PPG	0.00224
90S/10Z GA	0.00156
90S/10Z GA/GLY/PPG	0.00244

Here it can be seen that the material with GA present had the lowest coefficient, while the samples containing plasticizers had higher values. This shows that while the samples that contained crosslinker and plasticizer had a lower overall water uptake they still have a higher rate of diffusivity to water. Values for the samples without any additives could not be calculated as they did not reach a point of saturation during the tests.

### 3.5. Summary of Results

Compression molded samples consisting of soy and zein protein were produced and evaluated for mechanical properties, thermal stability, and water absorption. SEM images of fracture morphology were also obtained.

Initial processing at room temperature resulted in material with low compressive strength and modulus but did give insight on how to process with soy and zein protein. When this material was compression molded at elevated temperatures a material with improved morphology and mechanical properties

was achieved. This improvement was attributed to the plasticization and consolidation of the soy protein. The addition of zein to the material helped to keep the materials properties high even when plasticizers were added to it. The introduction of glutaraldehyde to the composite increased the compressive strength of the material to the highest attained value. It also increased thermally stability of the composite when compared against the plain material or material with plasticizers only as seen from the TGA results. SEM images show that the plasticizers helped with the consolidation of the proteins during processing. They also show that the samples break in a very brittle nature during fracture. Finally water absorption tests show that this material is very hydrophilic as the minimum amount of water absorbed was 100% of the starting mass. These tests also show that the water uptake rate and overall absorption was improved with the addition of plasticizers and crosslinkers. This is thought to be due to the improved consolidation of the proteins with addition of these materials. Additional studies into the processing and testing of this material may result in an improved material that would be suitable to replace currently used polymers in some application areas.

## CHAPTER 4. DDGS AND ZEIN PROTEIN COMPOSITES

### 4.1. Introduction

The residual of DDGS after oil and zein extraction comprises mostly of cellulose fibers/particles, which is a commonly used filler or reinforcement material in polymer composites. This chapter discusses studies conducted to use zein as an adhesive material to bind the cellulose particles together to form a composite. Doing this would also provide another use for DDGS and may be able to increase its value again. This material could potentially replace low performance synthetic polymers, such as low density poly(ethylene) (LDPE) or poly(propylene) (PP), in non-structural indoor uses. The biodegradability of the material could make it useful in areas such as pots for plants. Once a consumer buys a plant in this pot they would be able to put everything in the ground as the composite would decompose.

### 4.2. Materials and Methods

#### 4.2.1. Materials

DDGS was obtained from Tharaldson Ethanol plant (Casselton, ND); the material was ground using a z-mill and .25 mm mesh screen. Poly (propylene glycol) (PPG) 400 MW was obtained from Alfa Aesar (Ward Hill, MA). Glycerol was obtained from Mallinckrodt Chemicals (Phillipsburg, NJ). Corn zein (F-4000) was obtained from Freeman Industries (Tuckahoe, NY). Glutaraldehyde (GA) 50% was purchased from Fisher (Pittsburgh, PA).

#### 4.2.2. Processing

Commercial zein was dissolved in 80% ethanol and 20% water solution. After allowing that to dissolve DDGS that had both oils and zein extracted from it was added and allowed to mix thoroughly. When enough time passed to ensure thorough mixing extra ethanol was added till the solution was above 95 % ethanol, this would enable the zein to precipitate out and coat the DDGS

particles. This was then followed by decanting off the excess ethanol and placing the material in the compression mold. Both platens of the hydraulic press were raised to a temperature of 130 °C. The mold was then placed in the press and a slight pressure was applied for 30 minutes. A load of 9.5 tons was applied to the mold for 30 minutes. After that the mold was removed and allowed to cool before the sample was removed. Two different ratio of DDGS to zein were used 85/15 and 90/10. Also PPG, glycerol, and a 1:3 ratio of glycerol and PPG were used all at 20% ratio (based on total sample dry weight). Glutaraldehyde was also added by itself and in combination with PPG and the 1:3 ratio at 3% ratio based on total sample dry weight also.

Finally one centimeter long boiled flax fibers (150-200 µm diameter) were added to the best performing material in four different weight percentages; 2, 5, 10, and 15%. The fibers were added at the same time as the DDGS particles but these mixtures were hand mixed, as stirring with a stir bar caused all the fibers to clump in the middle. After the zein was precipitated out and the extra ethanol was decanted off the material was placed in the mold and compression mold in the same manner as material without fibers.

#### **4.2.3. Mechanical Testing**

Tensile testing was conducted on an Instron tester (5567) following a modified ASTM D638. Samples were dog bone in shape and had dimensions of overall length and width of 50 and 6 mm, respectively. The gauge area had a length and width of 10 and 1.7 mm, respectively. These samples were first cut to the overall width and then the gauge area was sanded down using a Dremel to the proper size using a metal jig as a guide. The tester was equipped with a 2 KN load cell and a test speed of 1 mm/min was used. Three samples were tested for consistency.

#### **4.2.4. Thermal Testing**

Thermogravimetric analysis (TGA) was conducted to determine the materials thermal stability. A TA TGA-Q500 with matching software was used to for these tests. The temperature was ramped from room temperature to 700 °C at 20 °C/min. Nitrogen flow (60 ml/min) was provided during the testing.

#### **4.2.5. Water Absorption**

Rectangular pieces of the compression molded material (13.5x7 mm) were dried for at least 24 hours and then completely immersed in water over a 36 hour period. The samples were removed at 5, 10, 15, 30, 60, 120, 240, 480, 960, 1440, and finally at 1920 minutes and measured for mass change.

#### **4.2.6. Microscopy**

SEM imaging was conducted on fractured specimens to study its morphology. A JOEL SEM system (JSM-6490LV) operating at 10 KV was used. Sample surfaces were sputter coated with gold before the tests.

### **4.3. Results and Discussion**

#### **4.3.1. Tensile Testing Results**



Figure 4.1. Compression molded DDGS/zein material.

Figure 4.1 shows the results of compression molding the DDGS/zein material. Figure 4.2 shows the results of tensile testing on the different samples. The 85/15 DDGS/zein sample has a slightly higher strength before any additives were introduced when compared with the 90/10 DDGS/zein material, possibly due to better interfacial bonding at the higher zein concentration. The plasticizers had a varying effect with the glycerol decreasing the mechanical properties but the PPG increased them over that of the pure material. The 1:3 ratio had a median effect when compared to the glycerol and PPG. The GA caused a slight increase on the tensile properties when used by itself but with the introduction of PPG the properties jump dramatically. This significant increase was attributed to the combined effects of zein plasticization and crosslinking. The combination of the 1:3 ratio of plasticizers and the GA showed a negligible effect. All the 85/15 material with additives had improved properties over the 90/10 material, which is similar to how the soy/zein material performed.

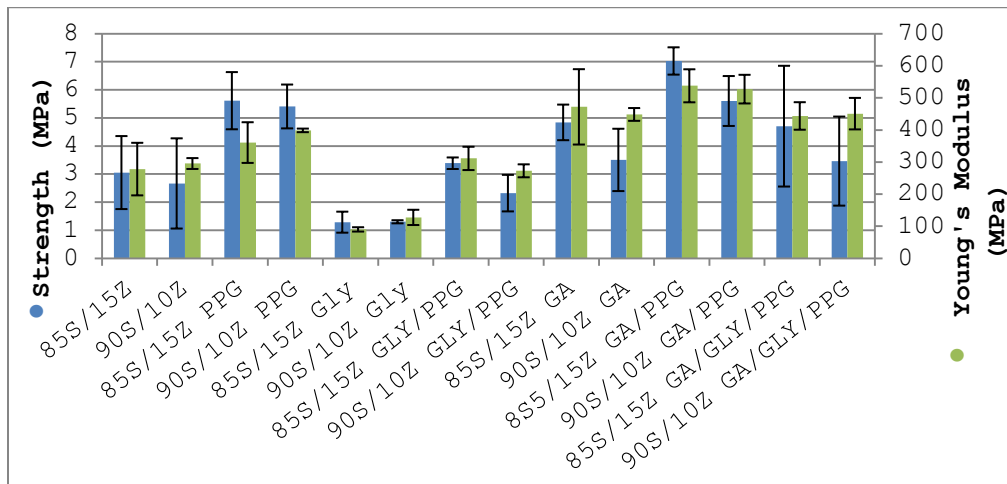


Figure 4.2. Strength and modulus values obtained from tensile testing of DDGS/zein composite materials.

Tensile testing results for DDGS/zein/Flax fiber composites are presented in Figure 4.3. The introduction of flax fibers to the DDGS/zein composites did not improve their mechanical properties. The 2 wt% materials did not contain enough fibers to help improve the properties, but as the weight percentage was increased the fibers were not homogeneously dispersed in the material thus causing material defects and stress concentration under load. Especially, when 15 wt% flax fibers were added, the defects and stress concentration led to a substantial decrease in the tensile strength. The non-uniform dispersion of the fibers was discussed in detail in section 4.3.3.

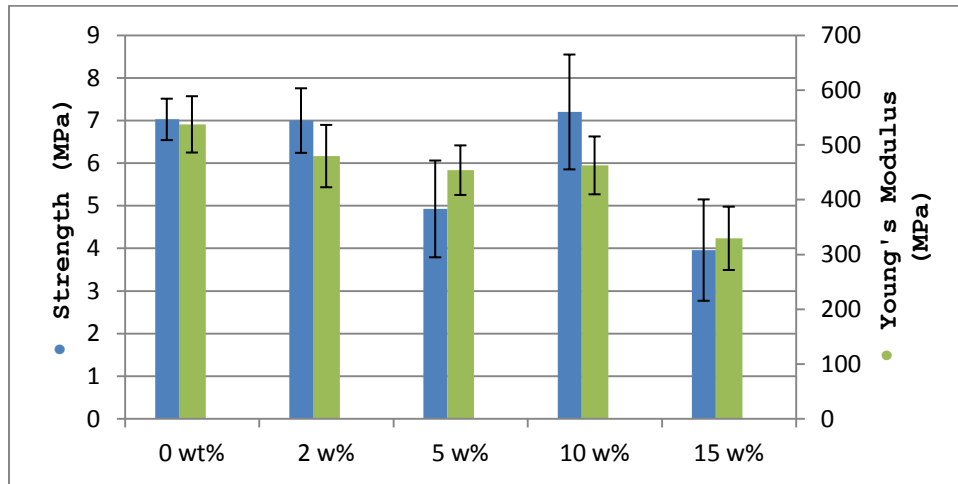


Figure 4.3. Strength and modulus values obtained from tensile testing of DDGS/zein/flax fiber composite materials.

Figure 4.4 shows representative stress-strain curves for the DDGS/zein composite materials. The addition of PPG alone increases the toughness of the material over that of the pure DDGS/zein composite. When GA is added along with the PPG the toughness is further increased due to a rise in maximum strength and maintained strain at break. Finally the addition of the flax fibers to try and improve the strength and modulus of the composite material did not achieve its purpose and reduced the toughness of the material at the same time.



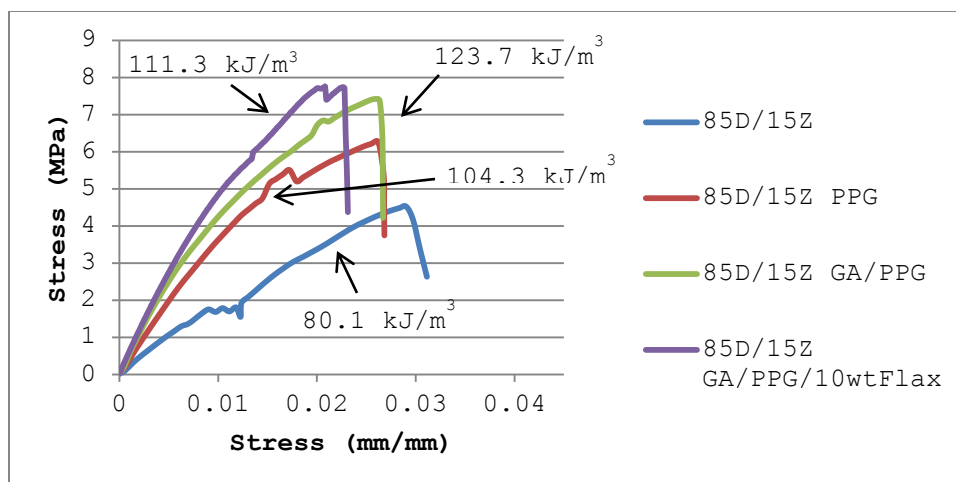


Figure 4.4. Representative stress and strain curves for DDGS/zein composite materials.

#### 4.3.2. Thermogravimetric Results

TGA results are presented in Figure 4.5 and significant values are in Table 4.1. Here an increase in initial degradation temperature (IDT) can be observed for all samples with additives. Both the samples containing PPG and GA had the highest IDT. The introduction of PPG and the 1:3 ratio to GA decreased IDT some. The two other plasticizers decreased the IDT when compared to the highest value. Again all samples with additives had smaller weight losses and they all had higher residual weight. This was due to their plasticizing and crosslinking effects on the zein adhesive, which helped to consolidate the samples and thus hindered mass and volatile transfer during thermal degradation.

Table 4.1: TGA Results for Initial Degradation Temperature (IDT), Percent Weight Loss, and Residual Weight of DDGS/Zein Composites.

Sample ID	IDT (°C)	Weight Loss (%)	Residual Weight (%)
85/15 Plain	147	65	12
85/15 PPG	226	58	20
85/15 GLY	208	55	20
85/15 1:3	209	58	21
85/15 GA	229	54	19
85/15 GA + PPG	212	55	19
85/15 GA + 1:3	216	52	19

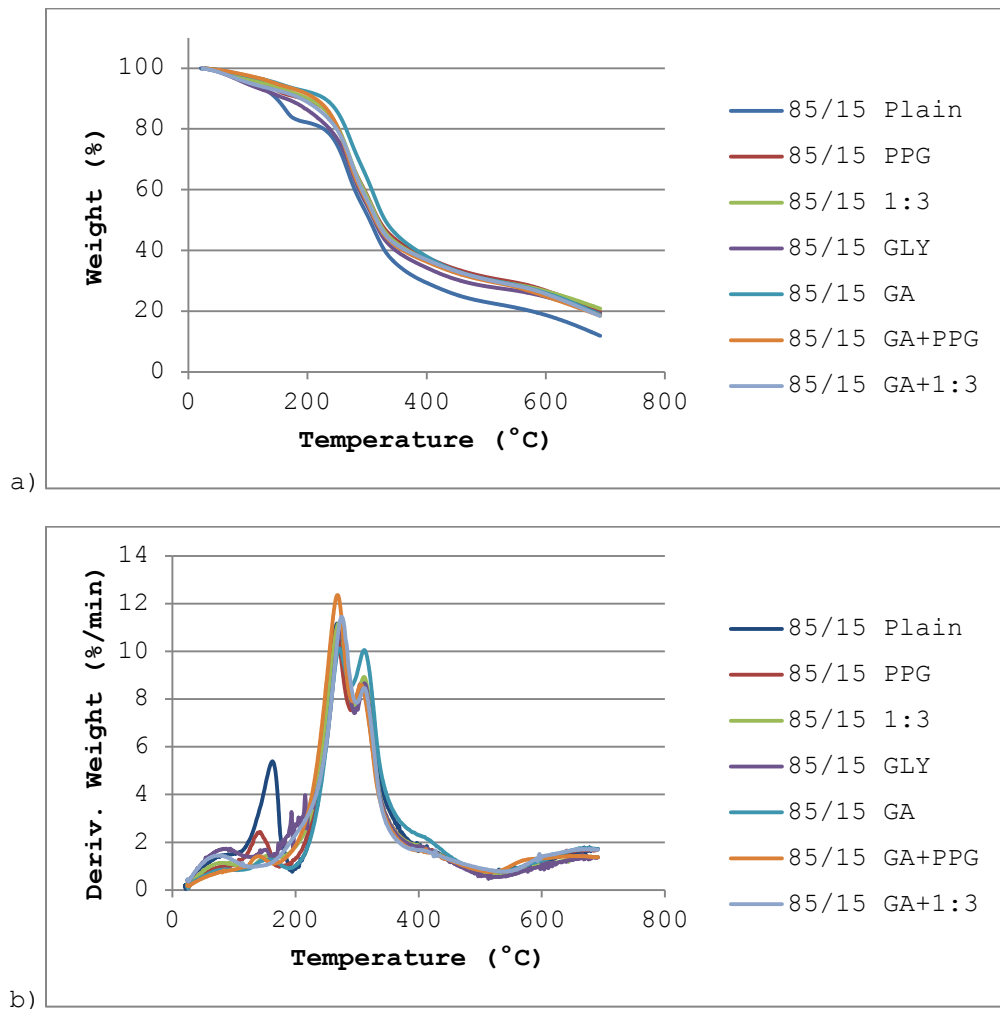


Figure 4.5. TGA and dTGA curves for DDGS/zein composite materials.

### 4.3.3. Microscopy

#### 4.3.3.1. DDGS/Zein Microscopy

Figure 4.6 shows the fracture surfaces for 85/15 DDGS/zein plain sample (a), with glycerol (b), with PPG (c), and with PPG and GA (d). The plain sample appears to have good bonding between zein and the DDGS particles. The sample with glycerol shows worsened bonding and consolidation, which explains its decreased mechanical properties. The sample with PPG improved

consolidation and the condition is further improved for the sample with PPG+GA, corresponding to the increase of their mechanical properties.

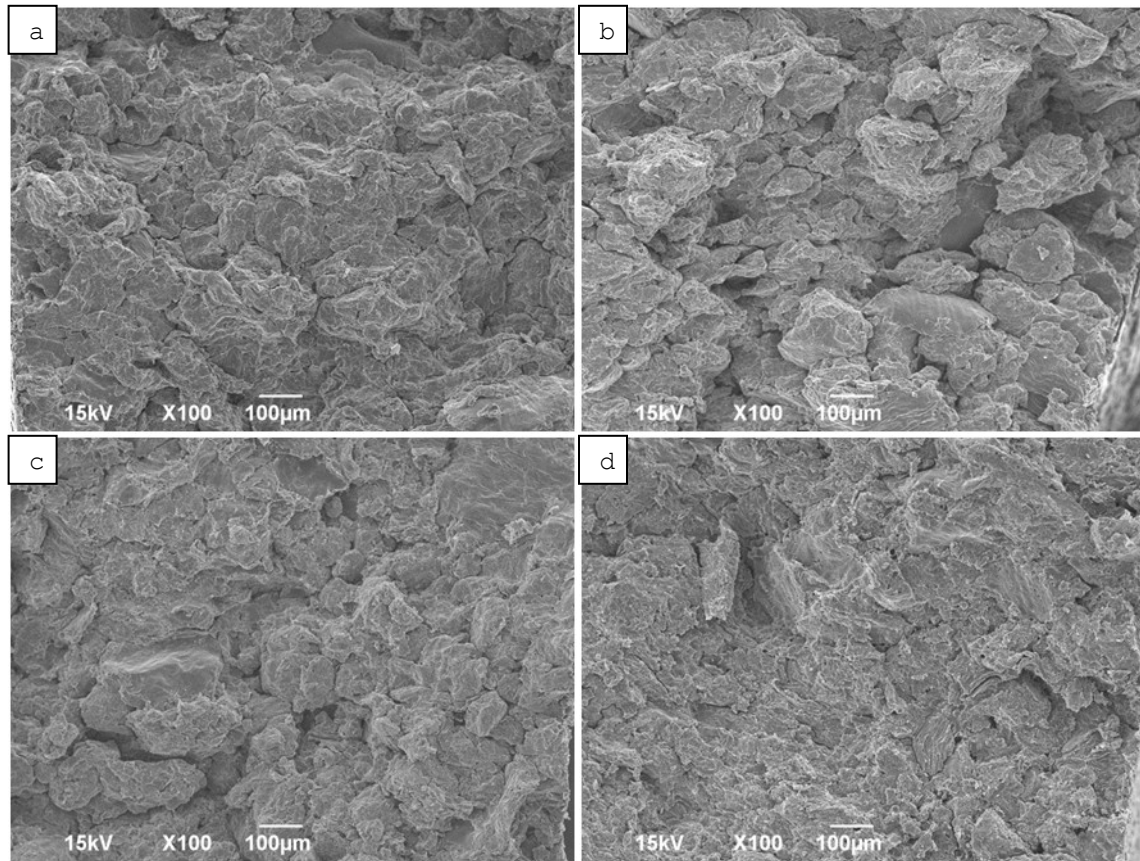


Figure 4.6. SEM images showing fracture surfaces of an 85/15 DDGS/zein (a), 85/15 + Glycerol (b), 85/15 + PPG (c), and 85/15 + PPG + GA (d).

#### 4.3.3.2. Flax Fiber DDGS/Zein Composite Microscopy

A and c of Figure 4.7 show the SEM images of fracture surfaces for the 15 w% flax fiber DDGS/zein composite, while b and d of Figure 4.7 show images for 2 w% flax fiber DDGS/zein composite. It can be seen that the fibers in the 15 w% material are not homogenously dispersed, but instead are concentrated to the left side of the sample. Also it appears the fibers are not being covered by the zein protein, which is supposed to bond the fibers and DDGS particles. A small amount of fibers are shown on the fracture

surface of the 2 w% material. For this material the fibers do show that zein has coated the flax fibers.

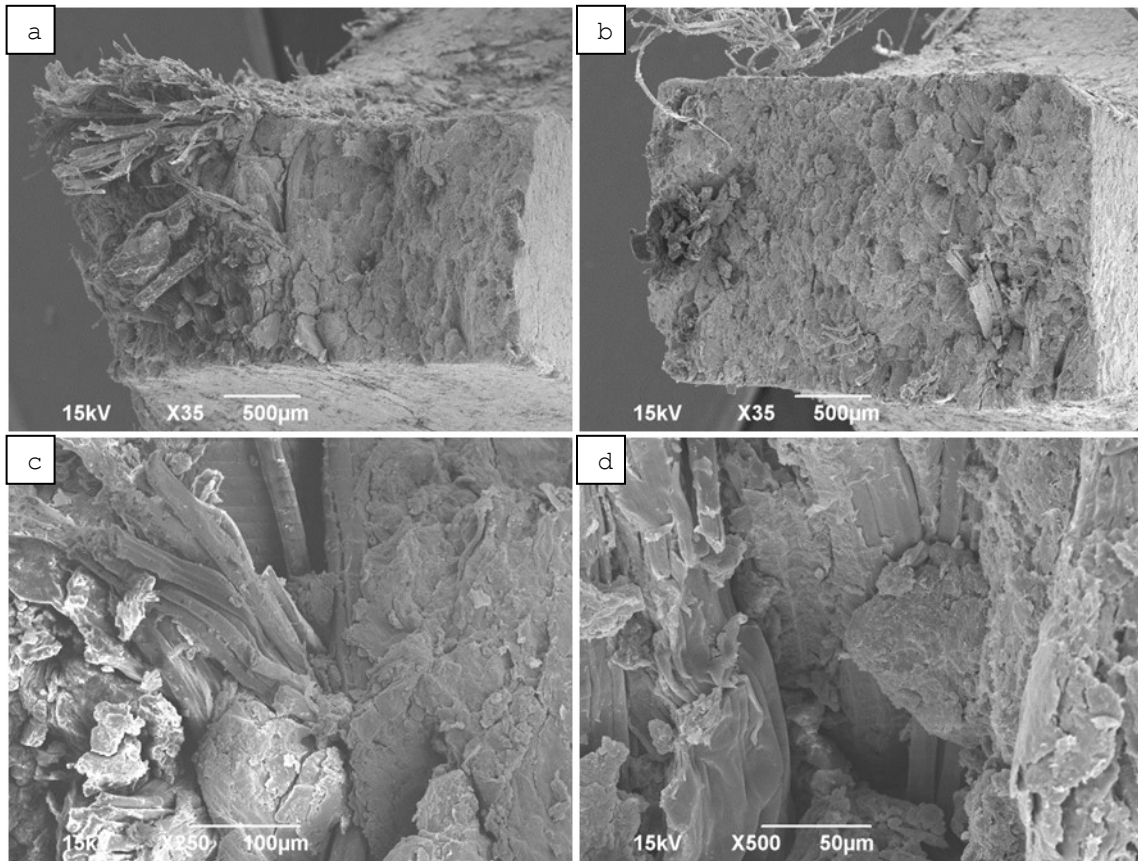


Figure 4.7. SEM images of fracture surfaces from DDGS/Zein/Flax fiber composites. a) 15wt% flax fiber b) 2wt% flax fiber c) 15 wt% flax fiber d) 2wt% flax fiber and samples were 85D/15Z+PPG+GA.

#### 4.3.4. Water Absorption Results

##### 4.3.4.1. DDGS/Zein Composite Water Absorption

Figure 4.8 below shows data attained during water absorption testing of DDGS/zein composite materials. As most tests resulted in the material dissolving and falling apart during the first few minutes of the test these values only show that these composites are not a water resistant material. The dissolution of the material is due to the remaining solubles in the DDGS and the in-ability of zein to completely coat all the particles to protect them from water attack. Many samples contained notches or cracks on the

surfaces which allowed water to penetrate the material at an elevated rate and thus hasten the dissolution. Reducing the number of surface cracks was found to be able to effectively decrease water absorption rates. Excluding the contributions from the surface cracks, the plasticizers and crosslinker do show effects on reducing water absorption.

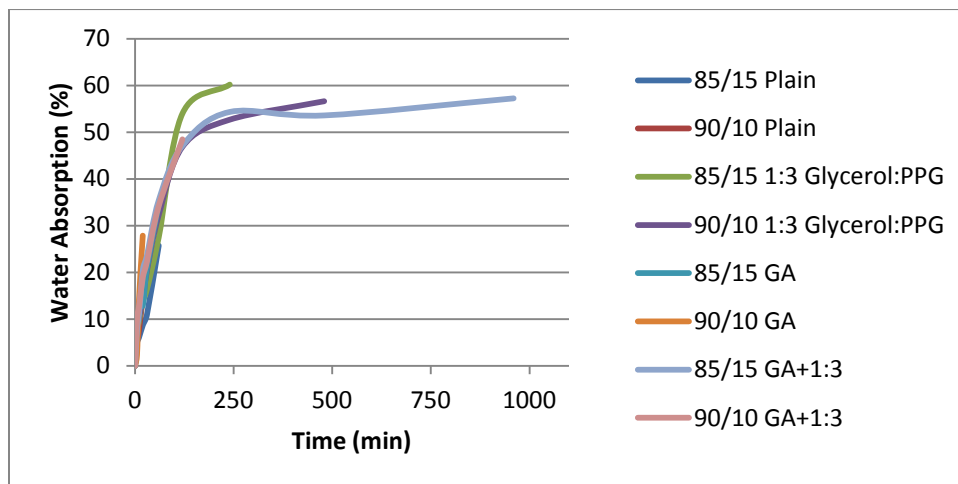


Figure 4.8. Water absorption vs. time curves for DDGS/zein composite material.

#### 4.3.4.2. Flax Fiber DDGS/Zein Composite Water Absorption

Water uptake data for flax fiber DDGS/zein composite materials is shown in Figure 4.9. Both the 2 and 10 w% composites had slower water absorption rates and lasted longer before deteriorating and becoming structurally unsound. While, both the 5 and 15 w% samples absorbed water at a faster rate and failed sooner. This is believed to be due to the sample defects caused by non-uniform dispersion of the fibers, which allowed water to infiltrate the sample and thus increased absorption and expansion of the samples.

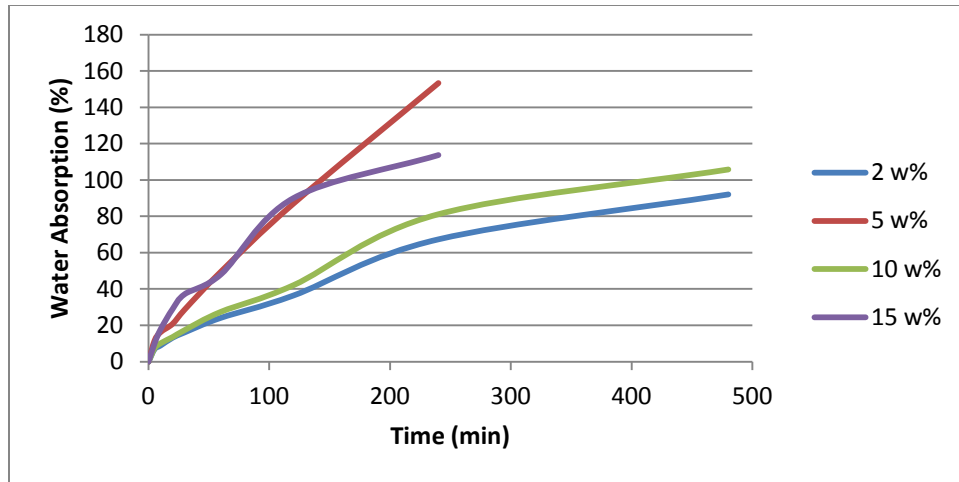


Figure 4.9. Water absorption vs. time curves for DDGS/zein composite materials containing flax fibers.

#### 4.4. Summary of Results

Compression molded composite samples consisting of DDGS and zein were created. Flax fibers were also added to try and improve the composites properties. These materials were then tested for mechanical properties, thermal stability and water absorption characteristics using tensile testing, TGA, and water emersion testing. Finally SEM imaging was conducted to study the morphology of fracture surfaces.

Tensile testing conducted on samples without any flax fibers showed low strength and modulus values. The inclusion of PPG and GA helped increase these properties to their maximum values; this is attributed to the improved plasticization and consolidation provided by the additives. The addition of glycerol had the greatest reduction on strength and modulus; SEM images showed that when glycerol was added the samples were not bonded well. Samples with the increased amount of zein provided superior performance over samples with reduced zein content, which is due to the extra zein increasing the bonding between the particles.

The addition of flax fibers to the DDGS/zein composite material had negligible effects on the tensile properties of the samples. This is attributed to either not enough fibers to help improve the materials performance or to the non-homogenous dispersion of the fibers. This resulted in material defects and stress concentrations during loading.

Introduction of additives to the material increased the composites thermal stability. GA increased the initial degradation temperature (IDT) to the largest degree. Residual material was consistent for all of the samples except for the pure DDGS/zein composite. The increase in IDT and residual material is credited to the increased consolidation and chemical bonding provided by the additives.

SEM imaging shows that better cohesion was achieved with addition of both PPG and GA to the DDGS/zein composite. Also the addition of glycerol seemed to reduce fusion between particles, while PPG improved it. SEM images of DDGS/zein/flax fiber composites show either there was not enough fibers in the samples to improve mechanical performance or there is so much fiber that the sample becomes unbalanced.

Water absorption testing of DDGS/zein composites show this material has too many remaining water soluble portions from the DDGS to even attain reliable tests. Introduction of the flax fibers does help to produce a composite that is more water resistant and allowed for increased testing times. Here again if the samples contained a crack or notch, they would allow water easier access to the interior and reduced the length of time before failure.

## CHAPTER 5. CONCLUSION AND FUTURE WORK

DDGS is the low value residual after corn ethanol fermentation which is mostly used as animal feed. Developing industrial uses of DDGS is expected to add value to corn products and reduce the cost of corn ethanol. DDGS comprises three major components including corn oil, zein protein, and cellulose and other carbohydrates. This research sought to maximize the industrial uses of DDGS via developing adhesive and composites using its zein and cellulose components.

The three major components, i.e., corn oil, zein, and cellulose were first separated from DDGS through ethanol extraction. Corn oil was first extracted using absolute ethanol under different extraction temperatures and times. A maximum of 21.3% oils were obtained at 70 °C within thirty minutes. The DDGS after oil extraction was further extracted for zein using 80% ethanol. A maximum yield of 18.6% was obtained at 70 °C when sodium sulfite was used to facilitate zein solution. Since in both extractions ethanol was used as the solvent, the processes can be done on-site in a corn ethanol plant, thus creating two additional value-added products from the plant. The residual of DDGS after the oil and zein removals were relatively pure cellulose, which can be used as a composite material.

Zein solution in ethanol was further studied as an adhesive material. CNF was added as a rheology modifier and a reinforcement agent for the adhesive. The addition of 1% CNF substantially increased the viscosity and dynamic moduli of the solution, thus making it an effective rheology modifier. CNF also markedly increased the strength and modulus of the zein adhesive. The increases were attributed to better mechanical interlocking of the adhesive with the surface of the wood and to the reinforcement the nanofibrils provided to the adhesive.



Zein was also studied as a constituent material in two composites: soy protein isolate (SPI)/zein and DDGS/zein. SPI/zein composites were compression molded at room and elevated temperatures. A maximum strength around 26.5 MPa and a modulus 0.9 GPa were obtained for the composite molded at room temperature. The strength and modulus were doubled for the composite molded at elevated temperature (130 °C). The increases were due to improved soy protein plasticization and consolidation. The addition of plasticizers to the composites showed mixed results while adding glutaraldehyde (GA) as a crosslinker increased the strength of the material. GA was also shown to increase thermal stability and water resistance of the composite.

The residual of DDGS after the oil and zein removals was blended with zein to make composites. DDGS/zein composites were prepared using a similar compression molding method. The addition of plasticizer PPG to the composite increased its tensile strength and modulus. This increase was attributed to the improve consolidation provided by the PPG. GA as a crosslinking agent also caused increases in both properties. When GA and PPG were added simultaneously, the composite achieved its maximum strength and modulus of 7 MPa and 0.5 GPa, respectively. Strengthening the composite with flax fiber was attempted without achieving obvious property improvement. The reason was due to inhomogeneous dispersion of the fibers. DDGS/zein and DDGS/zein/flax composites showed reduced water resistance compared to SPI/zein, possibly due to the strong hydrophilicity of DDGS and the flax fiber.

### **5.1. Future Work**

The work in this thesis was conducted to understand the extraction of corn oil and zein from DDGS under conditions that would be viable on site at an ethanol plant. This was then followed by determining how to process with the zein protein and residual DDGS to create other uses of adhesives and

composites. The removal of the oil and zein from DDGS was shown to be a viable option. Further research into scaling up this process to industry levels is needed to determine if it will remain a viable solution. Also determination of the exact composition of the extracts is needed, along with molecular weights the zein extract. Zein protein wood adhesives were created and provided decent properties but were still inferior to retail wood glues. There is a potential for this material to produce an adhesive that could compete with the retail wood glues. Additional studies that should be conducted to improve upon adhesion strength include increasing the CNF concentration in the adhesives and modifying plasticizer and crosslinker concentrations. Finally the DDGS/zein showed properties inferior to most plastics and currently only has the benefit of being biodegradable. Further work on this material to increase its performance includes changing current additive concentrations and using new additives.

## REFERENCES

1. WISNER R. Estimated U.S. Dried Distillers Grains with Solubles (DDGS) Production and Use. Ames IA. U.S. Department of Agriculture (USDA). 2012 Mar. 5 p.
2. MCFARLAND K. Eastern Corn Belt Ethanol Plant Report. Springfield IL. USDA-IL Department of Agriculture Market News. 2012 Apr. 1 p.
3. LI Y, and SUN X.S. Mechanical and Thermal Properties of Biocomposites from Poly (lactic Acid) and DDGS. Journal of Applied Polymer Science 2011; 121: 589-97.
4. SHUKLA R, CHERYAN M. Zein: The Industrial Protein from Corn. Industrial Crops and Products 2001; 13: 171-192.
5. SINGH N, CHERYAN M. Extraction of Oil From Corn Distillers Dried Grains with Solubles. American Society of Agricultural Engineering 1998; 41 (6): 1775-1777.
6. KWIATKOWSKI JR, CHERYAN M. Extraction of Oil from Ground Corn Using Ethanol. Journal of the American Oil Chemists' Society 2002; 79 (8): 825-830.
7. KWIATKOWSKI JR. Extraction of Oil from Ground Corn Using Ethanol. M.S. Thesis. University of Illinois at Urbana-Champaign; 2001.
8. SELLING G.W, and WOODS K.K. Improved Isolation of Zein from Corn Gluten Meal Using Acetic Acid and Isolate Characterization as Solvent. Cereal Chemistry 2008; 85 (2): 202-206.
9. XU W, REDDY N, and YANG Y. An Acidic Method of Zein Extraction from DDGS. Journal of Agricultural and Food Chemistry 2007; 55: 6279-6284.
10. PARRIS N, DICKEY L.C. Extraction and Solubility Characteristics of Zein Proteins from Dry-Milled Corn. Journal of Agricultural and Food Chemistry 2001; 49 (8): 3757-3760.

11. LAWTON J.W. Isolation of Zein Using 100% Ethanol. *Cereal Chemistry* 2006; 83 (5): 565-568.
12. KIM S, XU J. Aggregate Formation of Zein and Its Structural Inversion in Aqueous Ethanol. *Journal of Cereal Science* 2008; 47: 1-5.
13. ARGOS P, PEDERSENFL K, MARKSL M.D, LARKINS B.A. A Structural Model for Maize Zein Proteins. *The Journal of Biological Chemistry* 1982; 257 (17): 9984-9990.
14. GARRET R, OLIVA G, CARACELLI I, LEITE A, ARRUDA P. Studies of the Zein-Like  $\alpha$ -Prolamins Based on an Analysis of Amino Acid Sequences: Implications for Their Evolution and 3D Structure. *PROTEINS: Structure, Function, and Genetics* 1993; 15 (1): 88-99.
15. MATSUSHIMA N, DANNO G, TAKEZAWA H, IZUMI Y. Three-dimensional Structure of Maize  $\alpha$ -proteins Studied by Small-angle X-ray Scattering. *Biochimica et Biophysica Acta* 1997; 1339: 14-22.
16. PARRIS N, COFFIN D.R. Composition Factors Affecting the Water Vapor Permeability and Tensile Properties of Hydrophobic Zein Films. *Journal of Agricultural and Food Chemistry* 1997; 45 (5): 1596-1599.
17. SPENCE K.E, JANE J, POMETTO III A.L. Dialdehyde Starch and Zein Plastic: Mechanical Properties and Biodegradability. *Journal of Environmental Polymer Degradation* 1995; 3 (2): 69-74.
18. STURKEN O. Composition of Matter. US2115240 (Patent) 1938.
19. PARRIS N, DICKEY LC. Adhesive Properties of Corn Zein Formulations on Glass Surfaces. *Journal of Agricultural and Food Chemistry* 2003; 51 (13): 3892-3894.
20. SELLING GW, SESSA DJ, and PALMQUIST DE. Effect of Water and Tri (Ethylene) Glycol on the Rheological Properties of Zein. *Polymer* 2004; 45: 4249-4255.

21. ZHANG B, LUO Y, and WANG Q. Effect of Acid and Base Treatments on Structural, Rheological, and Antioxidant Properties of  $\alpha$ -Zein. Food Chemistry 2011; 124: 210-220.
22. GERICKE M, SCHLUFTER K, LIEBERT T, HEINZE T, AND BUDTOVA T. Rheological Properties of Cellulose/Ionic Liquid Solutions: From Dilute to Concentrated States. Biomacromolecules 2009; 10 (5): 1188-1194.
23. WANG Q, YANG Y, CHEN X, and SHAO Z. Investigation of Rheological Properties and Conformation of Silk Fibroin in the Solution of AmimCl. Biomacromolecules 2012.
24. TATARA RA, SURAPARAJU S, and ROSENTRATER KA. Compression Molding of Phenolic resin and Corn-Based DDGS Blends. Journal of Polymers and the Environment 2007; 15: 89-95.
25. LI Y and SUN XS. Mechanical and Thermal Properties of Biocomposites from Poly (Lactic Acid) and DDGS. Journal of Applied Polymer Science 2011; 121: 589-597.
26. ZARRINBAKHS N, MISRA M, and MOHANTY AK. Biodegradable Green Composites from Distiller's Dried Grains with Solubles (DDGS) and a Polyhydroxy(butyrate-co-valerate) (PHBV)-Based Bioplastic. Macromolecular Materials and Engineering 2011; 296: 1035-1045.
27. JOHN MJ and ANANDJIWALA RD. Chemical Modification of Flax Reinforced Poly (Propylene) Composites. Composites: Part A 2009; 40: 442-448.
28. KIM S. Processing and Properties of Gluten/Zein Composite. Bioresource Technology 2008; 99: 2032-2036.
29. MO X, SUN XS, and WANG Y. Effects of Molding Temperature and Pressure on Properties of Soy Protein Polymers. Journal of Applied Polymer Science 1999; 73: 2595-2602.

30. PAETAU I, CHEN CZ, and JANE JL. Biodegradable Plastic Made from Soybean Products. 1. Effect of Preparation on Mechanical Properties and Water Absorption. Industrial and Engineering Chemistry Research 1994; 33: 1821-1827.
31. CHABBA S and NETRAVALI AN. 'Green' Composites Part 1: Characterization of Flax Fabric and Glutaraldehyde Modified Soy Protein Concentrate Composites. Journal of Materials Science 2005; 40: 6263-6273.
32. WANG Y, CAO X, and ZHANG L. Effects of Cellulose Whiskers on Properties of Soy Protein Thermoplastics. Macromolecular Bioscience 2006; 6: 524-531.
33. COOKMAN DJ and GLATZ CE. Extraction of Protein from Distiller's Grain. Bioresource Technology 2009; 100: 2012-2017.
34. MIGNEAULT I, DARTIQUENAVE C, BERTRAND MJ, AND WALDRON KC. Glutaraldehyde: Behavior in Aqueous Solution, Reaction with Proteins, and Application to Enzyme Crosslinking. BioTechniques 2004; 37: 790-802.
35. SCHMIDT V, GIACOMELLI C, and SOLDI V. Thermal Stability of Films formed by Soy Protein Isolate - Sodium Dodecyl Sulfate. Polymer Degradation and Stability 2005; 87: 25-31.
36. OTAIGBE JU, GOEL H, BABCOCK T, and JANE J. Processability and Properties of Biodegradable Plastics Made from Agricultural Biopolymers 1999; 31: 56-71.
37. CHEN P and ZHANG L. Interaction and Properties of Highly Exfoliated Soy Protein/Montmorillonite Nanocomposites 2006; 7 (6): 1700-1706.
38. ANDERSON SP. Wood Fiber Reinforced Bacterial Biocomposites: Effects of Interfacial Modifiers and Processing on Mechanical and Physical

Properties [Master's Thesis]. Pullman, WA: Washington State University;  
Dec, 2007.

## **APPENDIX. OIL AND ZEIN EXTRACTION FROM DDGS**

### **A.1. Introduction**

The removal of any oils or fats that exist in DDGS could help improve the properties of a composite material created from DDGS. This could also create an additional byproduct in the form of the corn oil that would be removed. Since DDGS has zein protein in it, the removal of zein from DDGS would help create its own source of binder for composite materials. A plant producing ethanol could potentially remove the oils and zein protein all on location.

In this chapter the objective was to remove oils and fats from DDGS with the use of anhydrous ethanol. Also the extraction of zein protein from that de-fatted DDGS by the addition of aqueous ethanol. For all extractions were allowed to proceed for 120 minutes with varying shorter intervals. Also temperature was varied between 25 and 70 °C.

### **A.2. Materials and Methods**

#### **A.2.1. Materials**

DDGS was obtained from Tharaldson Ethanol plant (Casselton, ND); the material was ground using a z-mill and .25 mm mesh screen. DI water and absolute ethanol were obtained from our own stock room. Sodium Sulfite (SS) was purchased from Sigma Aldrich (St. Louis, MO).

#### **A.2.2. Processing**

##### **A.2.2.1. Oil Extraction**

The first attempt at removal of oils and fats from DDGS was conducted in a soxhlet extractor. This was chosen initially as the extraction method because it is an extremely efficient method but was later ruled out due to little control over parameters. Also trying to upscale this method to industry levels would be difficult.



Extraction of oils and fats were instead conducted in small batch extractions as a large mixer was not in our possession. Absolute ethanol was placed in a 60 ml sealable container, to help reduce evaporation losses, and placed on a hot plate. The ethanol was heated to 25, 50, or 70 °C before putting the DDGS in the container. DDGS was placed in an 80 °C oven overnight before being added to the solvent. After the DDGS was added the mixture was stirred for 2, 5, 15, 30, or 120 minutes. The solvent to solid ratio was held to 6 ml of ethanol/ g of DDGS, this value was based of experiments conducted by Singh and Cheryan<sup>5</sup>. After being stirred for the designated periods of time the mixture was removed from the hot plate and the DDGS was filtered out and placed in an oven at 80 °C overnight to dry. These remaining solids were weighed to determine total oil and fat removal. Each sample was repeated twice for consistency.

#### **A.2.2.2. Zein Extraction**

Extraction of zein was carried out in the same manner as the oils and fats. The ethanol solvent used for this extraction was 70% ethanol instead of absolute. This was placed in a sealable container and placed on a hot plate. This solution was then heated to 25, 50, and 70 °C before placing the de-fatted DDGS (DDGS residual from oil extraction tests) in it. After adding the DDGS the mixture was stirred for 10, 20, 30, 60, and 120 minutes. Solvent to solid ratio this time was held to 8 ml of solvent/ g of DDGS. When the time was completed the DDGS was filtered off and dried in an oven at 80 °C. The residuals were then weighed after overnight drying. As in the oil extraction each test was repeated twice for consistency. Optimal extraction conditions were determined from the above tests. 0.25 g of sodium sulfite, which is supposed to sever di-sulfide bonds of the zein protein and increase the

solubility, was added during extractions to evaluate its effects on the extraction results.

### A.3. Results and Discussion

#### A.3.1. Oil Extraction Results

The oil extraction results are presented in Figure A1. Extractions conducted at 25 °C had little change over time and was probably due to low solubility of oil in the solvent at this temperature. The extractions performed at 50 °C also showed insignificant variation within 30 minutes but when approaching 120 minutes a gradual increase in zein extraction was observed. Finally at 70 °C extractions exhibited a rapid increase within the first 30 minutes. As the process time increased the extraction leveled off till the end of the tests. Oil extractions at the end of 30 minute extraction times were 13.4, 14, and 21.3% for 25, 50, and 70 °C, respectively. Based on Figure 6 the extractions conducted at 70 °C were the most efficient as the highest amount of oil was extracted in the shortest period of time.

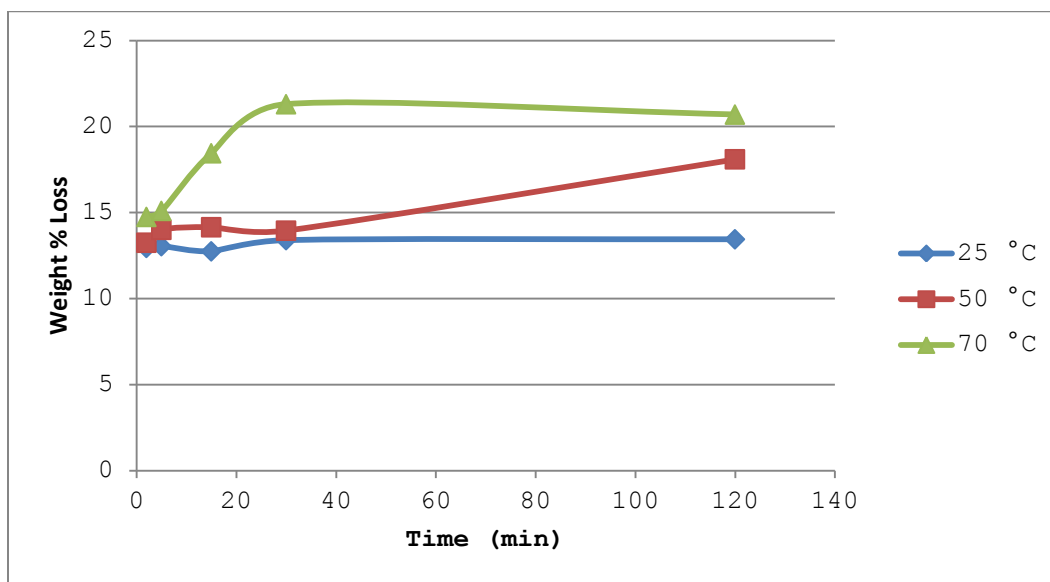


Figure A1. Oil extractions as functions of time and temperature.

### A.3.2. Zein Extraction Results

Zein extraction results are presented in Figure A2. The extractions conducted at 25 °C showed minimal increase in zein removal within the 120 minute long tests. At 50 °C, the removal of zein was slightly higher but did not vary substantially over time. The 70 °C extractions increased with increasing process time and were the highest among the three temperatures used.

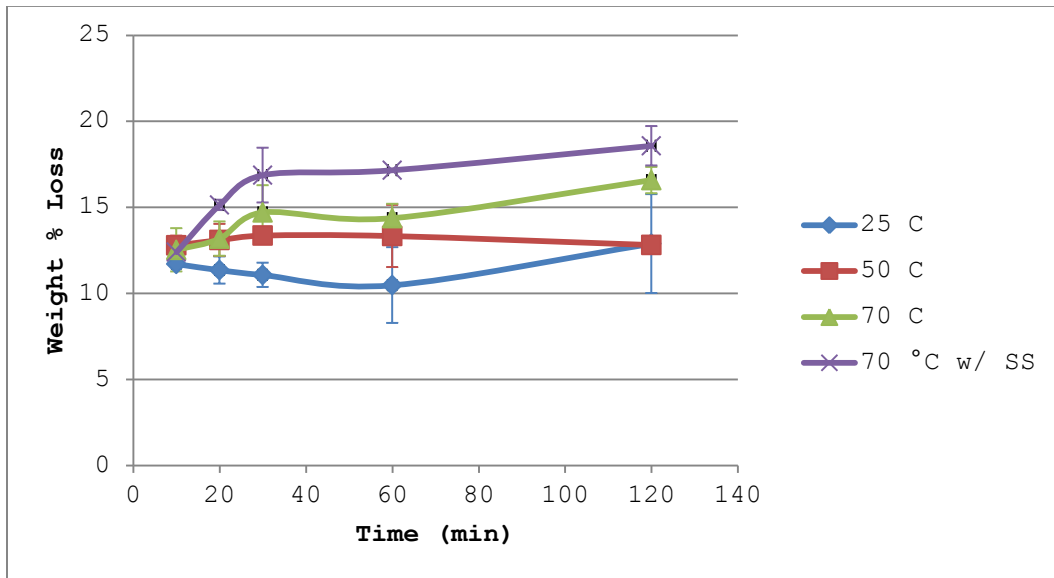


Figure A2. Zein extractions as functions of time and temperature.

The addition of sodium sulfite caused an increase in zein extracted. Parris and Dickey<sup>10</sup> used sodium sulfite (SS) to obtain similar results of a slight increase in the amount of protein extracted. The increase in the extraction is attributed to some of the proteins containing disulfide bonds. Sodium sulfite or sodium bisulfate, which was used by Cookman and Glatz<sup>33</sup> to help zein extractions, are capable of breaking these bonds. The maximum amount of zein protein extracted was 12.9, 13.4, 16.6, and 18.6% for 25, 50, 70 °C, and 70 °C with sodium sulfite, respectively.

#### **A.4. Summary of Results**

Corn oil was extracted from DDGS using absolute ethanol, under relatively easy operating conditions. A maximum of 21.3 oil yield was obtained during one extraction. Removing this oil from DDGS is expected to increase mechanical properties of DDGS based composites and the corn oil would be an additional byproduct. Zein protein was also extracted from DDGS using aqueous ethanol, with the maximum extraction of 18.6% of zein protein occurring at the highest temperature and longest time and with the addition of sodium sulfite. This removal of zein would create a new source of low-cost zein thus making it more viable for composites and adhesives.